

Response to Anonymous Referee #1

We thank the reviewer for their very detailed and insightful comments and suggestions. Below, we specifically answer each of the issues raised and provide information on how we suggest changing the manuscript accordingly. Accompanying this response letter, we provide a revised manuscript. In the revised manuscript we used blue font for the sections we suggest to change in response to the reviewers comment. Throughout this letter, we refer to page and line numbers of the revised manuscript.

This paper aims to further our understanding of the how electron transport rates (ETRs) are coupled to carbon fixation (i.e. CO₂ uptake rates), by examining the diurnal variability of the electron rate for carbon fixation (K_c) in the field. The authors directly compare ETR measurements against 14c-uptake for the first time throughout a diel cycle, a relevant goal with the potential to improve our capacity to derive primary productivity estimates from FRRF fluorometers. Similarly, the observed relationship between non-photochemical quenching (NPQ_{NSV}) and K_c may provide supporting evidence for their previous findings (Schuback et al. 2015) that this parameter may hold value as a predictor for this conversion factor. In spite of the positives, I believe that the viability of NPQ_{NSV} to predict K_c under varying environmental/taxonomic scenarios needs more attention from the authors; as it stands this paper does not really add a huge amount of value to their previous study for this reason. Given that taxonomic groups likely have different capacities for NPQ (and therefore potentially varying levels of reliance upon alternative electron pathways to relieve excitation pressure upon PSII) it needs to be considered how the dominance of particular groups may influence the NPQ signature relative to K_c. In other words, how widely do the authors expect their findings to hold across waters where taxonomy is changing?

The primary aim of the present study was to determine the presence and magnitude of diurnal variation in the coupling of photosynthetic electron transport and carbon fixation in iron-limited phytoplankton in the NE subarctic Pacific. Our results show significant uncoupling of the two rates over a diurnal cycle under conditions of iron limitation. This result is the key aspect of the paper, and its main contribution to the field. As pointed out by the reviewer, the new field data we present are the first of their kind, and should thus be of significant value to the community.

Our results further add to the large amount of experimental evidence which shows that a constant conversion factor cannot be used to derive rates of carbon fixation from FRRF derived rates of ETR. If, and how, the required conversion factor can be estimated with sufficient accuracy has become a major research question in the field (e.g. Lawrenz et al., 2013). Building on previously published work from the same oceanic region, we suggest that an observed empirical correlation of the derived conversion factor and NPQ_{NSV} holds promise to improve

approaches aimed at modeling a variable conversion factor. However, this is not the focus of the manuscript, and we fully recognize the potential limitations pointed out by the reviewer in relation to taxonomic and environmental variability. In the present manuscript, about half of the section describing the correlation between K_c and NPQ_{NSV} (section 4.4., pages 18824-16826) is dedicated to possible caveats, concluding with the sentence:

“Larger datasets, spanning multiple oceanic regions and phytoplankton assemblages of contrasting taxonomic composition and physiological state are needed to further investigate the correlation between NPQ_{NSV} and $\Phi_{e:c}/n_{PSII}$.”(section 4.4., pages 16826, lines 25-27)

We feel that this is a very clear statement of exactly the kind of caveats raised by the reviewer. In the revised version of the manuscript we have taken great care to further emphasise the preliminary nature of the approach.

Additionally, the authors have a reasonable argument that deriving [RCII] from a fluorescence-based algorithm (Oxborough, 2012) is problematic due to iron-limitation (and this is potentially due to a change in the quantum yield of fluorescence) so does /will their approach to reconcile K_c from NPQ_{NSV} still perform under iron-replete conditions (or indeed other environmental conditions that alter the quantum yield of fluorescence)?

As the reviewer points out, the Oxborough approach to quantify [RCII] from a fluorescence based algorithm is problematic under conditions of iron limitation. Working in an iron-limited region of the ocean, we thus combined the two unknown parameters into one conversion factor out of necessity, as opposed to undervaluation of the benefits gained from knowing [RCII]. In response to an insightful suggestion by reviewer #3, the revised version now contains estimates of the relative diurnal change in [RCII] (and $1/n_{PSII}$), which we use to deduce the contribution of diurnal changes in K_c to the 'lumped' conversion factor (page 11, lines 292-316; page 14, lines 380-390; page 17, lines 487-488,; page 18 494-497).

We have also emphasised that our results may be difficult to extrapolate to high iron regions (page 22, lines 626-629). Yet, given that vast regions of the contemporary surface ocean (about 30%) are affected by iron limitation, our approach is likely applicable to a significant fraction of surface ocean environments (see additional comments below).

By divorcing themselves from the requirement to quantify [RCII], this approach rests heavily on the ability to empirically relate NPQ_{NSV} and K_c in order to derive ecologically-relevant productivity rates from ETRs , so this needs to be robustly tested under different scenarios to determine its validity (can we really not consider the variability of n_{PSII} ?).

As discussed above, we now estimate relative changes in RCII, thus explicitly considering variability in this parameter. It is worth noting, however, that even with robust estimates of

[RCII], derivation of carbon-based productivity rates still dependent on an estimate of K_c , which is subject to significant variability. Indeed, our results show that most of the variability in the overall conversion factor is due to changes in K_c , rather than [RCII]. We are not aware of any robust approach which could estimate K_c on its own. Our results provide a potential approach (which may not work under all conditions) to estimate K_c/n_{PSII} from FRRF data and thereby estimate carbon-based productivity from FRRF data alone.

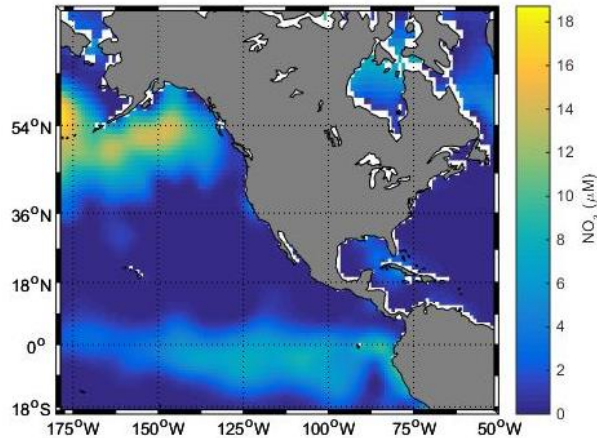
My main concern here is that not quantifying [RCII] the authors potentially advocate a “backwards step” for the field of active fluorometry (until the reliability of NPQNSV as a predictor of K_c is robustly evaluated) where the variability of n_{PSII} is not quantified. For this reason, the paper (and the robustness of the messages, and hence impact, the authors are trying to convey) would immensely benefit from an additional side-experiment using cultures (iron-replete preferably from a selection of taxa) to see how robust this approach is.

We agree that laboratory experiments are needed to further investigate the correlation between K_c/n_{PSII} and NPQ_{NSV} . However, these need to include a wide range of species and light as well as nutrient conditions and are not within the scope of the present manuscript.

Overall the approach to examine the diurnal variability of K_c does add to our existing understanding of the coupling of ETR to C-uptake (but would benefit from more commentary to discuss/infer upon the mechanisms that act to decouple the rates during periods of saturating light).

I remain less convinced about their advocating NPQNSV as a broad predictor of K_c due to the fact that it has been tested under a very specific environmental niche.

We are not advocating the relationship as a broad predictor of K_c . Yet, the data presented in this paper, in addition to that of Schuback et al. (2015), do show that the relationship appears to hold up well for the iron-limited subarctic Pacific. We disagree that this oceanic region represents a 'very specific environmental niche'. As shown in the Figure below, iron limited waters (defined by areas with excess summer time macro nutrients) cover large swath of the Eastern Subarctic Ocean. We can conservatively estimate the area to cover $\sim 1,500 \times 1,500$ km, which is equivalent to more than 2 million km^2 . This surface area far exceeds that of many other regions (e.g. North Sea) that have received significant research attention, and would not likely be considered as 'specific environmental niches'.



As mentioned above, we have revised the manuscript in order to emphasise the main focus of the present study (the uncoupling of ETR and carbon fixation over a diurnal cycle). We do share the reviewers' reservations about the applicability of a NPQ_{NSV} -based conversion factor across contrasting environmental and taxonomic regimes and we have revised the manuscript to further emphasise this (page 1, line 31; page 22, lines 621-623). We do, however, stand by our claim that the observed empirical correlation holds promise to improve approaches aimed at modeling the conversion factor and in turn improve estimates of carbon-based primary productivity from FRRF measurements.

I would encourage the authors to provide additional lab-based data to support this, or alternatively to critically evaluate the potential conditions where this relationship may break-down, in order that studies following on from this work can begin to systematically test this.

We revised the manuscript to tone down the potential of the observed correlation and address potential limitations of the approach. As mentioned above, we agree that lab studies are certainly needed. But, in order to fully validate the approach, one would require lab studies with many different species, different iron, light, nutrient levels etc. We are actually pursuing these in our group, but we need a comprehensive suite of measurements, and more than could be put into this paper.

Specific Comments

(16805 LN8) – I'm not convinced that the 1993 or 2004 papers cited are "more recently" (either amend the nature of this sentence or the references used to justify)

We were trying to convey the fact that active chlorophyll a fluorescence based methods are recent in relation to “traditional” incubation based methods including 14C-uptake studies. We have changed “More recently” to “Over the past two decades” (page 2, line 39).

(16805 LN23) – Hancke et al. (2015, PLoS One) recently proposed the symbol K_c is more appropriate to describe the “electron requirement for carbon fixation” following the (correct) logic that the symbol Φ widely denotes a quantum yield of a process, rather than a quantum requirement. The authors could also consider adopting this nomenclature to standardise terminology (which can often be confusing for non-specialists).

We have changed the nomenclature throughout the manuscript, and have explicitly noted the change in terminology with respect to our recent study (page 2, lines 52-53).

(16805 LN24) – “Plasticity in both parameters can be observed” this sentence needs to be supported by appropriate references and perhaps the range of variability encountered with each parameter (and hence what the scale of assuming $1/n_{PSII} \times \Phi_{P_{max}}$ amounts to).

We have added information on the range of variability encountered as $1.15 - 54.2 \text{ mol } e^- \text{ mol } C^{-1}$ for K_c (Lawrenz et al., 2013) and approx. $200 - 950 \text{ mol chl a mol } RCII^{-1}$ for $1/n_{PSII}$ (Suggett et al., 2010). Using these ranges, the conversion factor K_c/n_{PSII} could vary from $230 - 51490 \text{ mol } e^- \text{ mol } C^{-1} \text{ mol chl a mol } RCII^{-1}$ (page 11, lines 284-287).

The recent meta-analysis by Lawrenz et al., 2013 found a mean value of $11.8 \text{ mol } e^- \text{ mol } C^{-1}$ for K_c , while $500 \text{ mol chl a mol } RCII^{-1}$ is commonly assumed for $1/n_{PSII}$ (Kolber and Falkowski, 1993). Using these values, the conversion factor K_c/n_{PSII} would be $5900 \text{ mol } e^- \text{ mol } C^{-1} \text{ mol chl a mol } RCII^{-1}$, which is consistent with the range encountered in our study ($2700 - 9200 \text{ mol } e^- \text{ mol } C^{-1} \text{ mol chl a mol } RCII^{-1}$). These theoretical calculations were discussed in the original manuscript (page 16820, lines 19-23), and can be found in the revised version on (page 18, lines 490-493).

(16806 LN2-9) - The main concern with this paragraph is that it implies these past studies have examined this “conversion factor”, ATP/NADPH requirements as well as assimilation efficiencies – I don’t think this is the case and perhaps the authors need to consider more appropriate references or clarify exactly how these references support this statement.

We agree with the reviewer and have rewritten the sentence (page 3, lines 59-62).

Also, a slightly better description than “backpressure” is needed here – it is not explicit as to what the authors are referring to as an accumulation of electrons within the electron transport

chain (and/or subsequent effects upon intracellular reductant/ADP-ATP ratios etc). Perhaps also clarify that this “backpressure” is undesirable.

The section has been rewritten (page 3, lines 62-69).

(16806 LN13) - I guess another way of looking at this is that 14C P versus E data has a “classic” diurnal “hysteresis” to it. The question is whether ETRs also are affected in the same way (and/or to the same extent). I was not convinced that ETRRCII would be (effectively) independent of time of day (no hysteresis) since systems can easily build NPQ, RCII deactivation etc, which would cause much less efficient systems in the afternoon (increasing E) than afternoon (decreasing E). This sentence needs proper thought, clarification and appropriate support from past studies.

The whole paragraph has been removed from the introduction of the revised manuscript, and we now mention the likely diurnal hysteresis in ETR specifically in the discussion (page 17, lines 482-486).

(16806 LN19) - Agreed, but it may be useful to state that at best past FRRf studies have integrated ETR and C-uptake over entire diel scales (Suggett et al. 2006, Limnology & Oceanography) and thus the potential time-dependency remains unresolved.

We have changed the manuscript accordingly, referencing the study by Suggett et al., 2006 (page 3, lines 8-83).

(16808 LN6) – The authors state that 3 hours of PAR data is lost, which is understandable (if unfortunate) however I think it would be useful to clarify which 3-hour time period is missing from the dataset and has been extrapolated (for consideration when interpreting results).

The time period for which the PAR data was extrapolated (bases on continuously logged SW radiation data from the NOAA buoy) was 14:00 – 17:00. This has been clarified in the revised manuscript (page 5, lines 114).

(16809 LN8) – Perhaps justify why was pigment analysis was only performed at 4 time points? – Noon pigment samples would have been useful to look at photoprotective pigments rather than have a 6 hour gap (9am – 3pm).

We agree and, in light of the results, would love to have pigment data for all time-points. However, it was simply not feasible to collect samples at all time-points due to logistical

constraints (all of the measurements and sampling were conducted by two people). The revised manuscript acknowledges that higher resolution data would have been desirable (page 14, lines 394-395; page 15, line 413).

(16811 LN1) Because the authors are working with low biomass samples (0.2ug/l chl_a) is the averaging of 20 sequences adequate to reliably extract fluorescence parameters? (particularly at higher PAR levels). I know the Soliense is a capable instrument with high sensitivity so just a line or two confirming the authors have considered this would be useful.

If we just consider the last acquisition (average of 20 sequences) at each light level, the signal to noise ratio (S/N), calculated as the ratio of signal mean to signal standard deviation, is very high (approx. 400) for all parameters acquired during the dark and low background light levels of our light curves. As the reviewer points out, the S/N ratio of the derived parameters decreases at high background irradiances where the S/N for F' and F_m' is still above 200, but as low as 5 for σ' . The significant decrease in the S/N for σ' is to be expected, due to loss in variable fluorescence and therefore recovery of fit parameters. However, given that deriving ETR using calculations which include σ' (low S/N) as well as calculations which only use σ measured in the dark-regulated state (high S/N) give us very similar results (see answer to comment below), we are confident that σ' can be reliably extracted from 20 sequences.

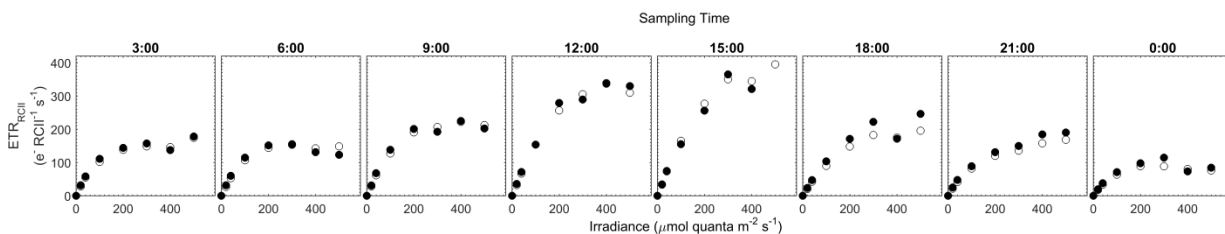
It is furthermore worth stressing that all derived parameters used for the ETR calculation are the mean of the last three fits, each of which is the average of 20 sequences.

(16811 LN17) - It might help to justify why the authors use $\sigma' \times F_q'/F_v'$ in eq 3 for the non-photochemical quenching/photochemical quenching components as opposed to $\sigma \times F_q'/F_m'$?

The two approaches may give different ETRRCII if not all NPQ is coming out of the antennae (e.g. RCII-bed quenching), which may be important under diel conditions where RCII are deactivating (e.g. Gorbunov et al. 2001 Limnology & Oceanography) – could this be why the ETR and 14C decouple under the diel scenario and perhaps an artefact of the ETR algorithm used. This may need some additional data analysis to rule out.

The two alternative approaches to calculate ETR described above are $ETR = E \times \sigma' \times F_q'/F_v'$ and $ETR = E \times \sigma \times (F_q'/F_m')/(F_v/F_m)$. The main difference between these approaches relates to how (and where in the equations) one accounts for the effects of non-photochemical quenching on measured ChlF yields. The two approaches are equivalent under conditions where non-photochemical quenching is caused by thermal dissipation of absorbed energy in the light harvesting antenna and $\sigma' = \sigma \times (F_q'/F_m')/(F_v/F_m)$ (Gorbunov et al., 2001).

As shown in the figure below, these two equations give very similar results. For all ETR_{RCII} values used in this study ($n=71$) the difference between values calculated in both ways ranged from 1 % to 16 % with a mean coefficient of variance of 6%. This information is now included in the manuscript (page 8, lines 216-221).



● $ETR = E \times \sigma'_{PSII} \times F_q' / F_v'$

○ $ETR = E \times \sigma_{PSII} \times (F_q' / F_m') / (F_v / F_m)$

(16811-16812) - Similarly, I see no mention of subtraction of background fluorescence, which could entirely influence the outcome on the derived fluorescence parameters (Cullen & Davis 2003) and in turn the F_q' / F_v' retrieval – was this performed? Given the low biomass this step could have an important impact upon derived fluorescence parameters, and contribute to the low F_v / F_m values recorded (if not performed), which would then carry through to F_o' and in turn F_q' / F_v' . The authors will need to carefully consider whether a lack of blank correction at each time/depth is contributing to the decoupling of ETR and ^{14}C uptake over time.

Blank corrections were performed for each sample and values for each wavelength automatically subtracted during the sample run. We added a description of the exact procedure for blank-correction in the revised methods section (page 7, lines 181-182).

(16811 LN23) – I think it makes more sense to specify that you are converting units of angstroms to m^2 rather than simply just 10-20 m^2 to m^2

We have used these units to be consistent with the editorial requirements (SI units) of the journal.

(16812 LN10) - It would be good to provide justification for the incubation time and briefly discuss, as an incubation of this length falls closer to NPP along the continuum of GPP – NPP compared to the (shorter) ETR measurements.

Less than 2 hr incubations would have potentially been too short to observe a meaningful signal, given the low growth rate, low biomass and small volume used. Since the diurnal sampling time-points were 3 hr apart, a 3.5 hr incubation time was necessary to spike and set up samples from one TP and then filter samples from the previous TP. In the revised methods section, we have now added some text (and two supporting references; Halsey et al., 2011; Pei and Laws, 2013) stating that our approach may approximate a rate closer to net rather than to gross carbon fixation (page 9, lines 244-246).

(16814 LN11) - It was not clear in this sentence “it is unlikely to give accurate results under conditions of iron limitation” why the following citations were used – have they explicitly tested the algorithm of Oxbrough to derive [RCII]? If not, why do the authors suspect the references provide the evidence that the [RCII] algorithm would not apply. Some serious justification and clarification is needed here.

The inherent assumption to the approach of Oxbrough et al. is that the ratio of the rate constants of photochemistry (k_p) and fluorescence (k_f) stay within a narrow range. This is not the case under iron limitation, where k_p decreases while k_f increases (e.g. Vassiliev et al., 1995). Indeed, the original paper by Oxbrough et al. cautioned that the approach relied on assumptions which might not hold under nutrient limitation, especially if the limiting nutrient is iron (Oxbrough et al., 2012). This potential caveat was recently repeated by Robinson et al., 2014, who say:

“The calculation of [RCII] using the relationship between the minimum fluorescence parameter (F_0) and [RCII] as determined by Oxbrough et al. (2012) may be sensitive to nutrient stress (C.M. Moore pers. comm.) which results in the enhanced uncoupling of chlorophyll complexes and PSII reaction centres (...).”

A recent publication by Silsbe et al. (2015) includes data for cultures grown without added iron, though no specific information is presented on the extent of iron limitation in these cultures. In the assessment of their data, Silsbe et al. note that:

“..., both Tp-Fe and Tw-Fe cultures grown in the absence of iron predicted higher [RCII] than measured. Consequently these cultures yielded lower K_R values than other cultures. This key finding is consistent with the concept that iron limited phytoplankton may accumulate a store of non-energetically coupled chlorophyll-binding complexes that increases the quantum yield of fluorescence (Φ_f) relative to iron replete phytoplankton (Behrenfeld and Milligan 2013; Macey et al. 2014). As K_R is proportional to Φ_P/Φ_f , an increase in Φ_f would diminish K_R as observed in this study. Omission of

these iron-deplete cultures generally increased the mean K_R value for each instrument and reduced its variance...”

In the revised manuscript we changed the wording to be less ambiguous about why we did not apply the Oxborough approach. We furthermore added a whole section in which we applied a simplified version of the Oxborough approach to quantify relative diurnal changes in $1/n_{PSII}$ (page 11, lines 292-316; page 14, lines 380-390; page 17, lines 487-488; page 18 494-497).

(16814 LN16) I think that if the authors differentiated parameters by using the nomenclature P_{max} to refer to maximum carbon uptake rates, and ETR_{max} (which is more in line with convention and specific to the measurements from which the parameter is derived) when referring to maximum electron transport it would avoid any possible confusion between the terms (e.g P_{max} of ETR) (this issue also applies to the previous paragraph where deriving “ P_{max} ”).

We changed the abbreviations used in the text to $P_{max-ETR_{RCII}}$ and P_{max-C} as well as $\alpha-ETR_{RCII}$ and $\alpha-C$.

(16817 LN22) I feel that the authors are definitely stating that PPC is highest at noon, when in fact this timepoint was not sampled, and the data between 9am-3pm has been extrapolated. This could be phrased better to include the potential element of uncertainty in this statement.

We did not mean to imply mid day as the strict noon hour, and have clarified the sentence (page 14, lines 399-401).

(16818 LN7) Typo – should read “in-situ 5m irradiance”.

We clarified, that, like throughout the manuscript, in situ irradiance refers to irradiance at 5 m depth (page 15, line 425).

(16818 LN28) Typo – should read de-epoxidation (not de-epoxilation)

Corrected.

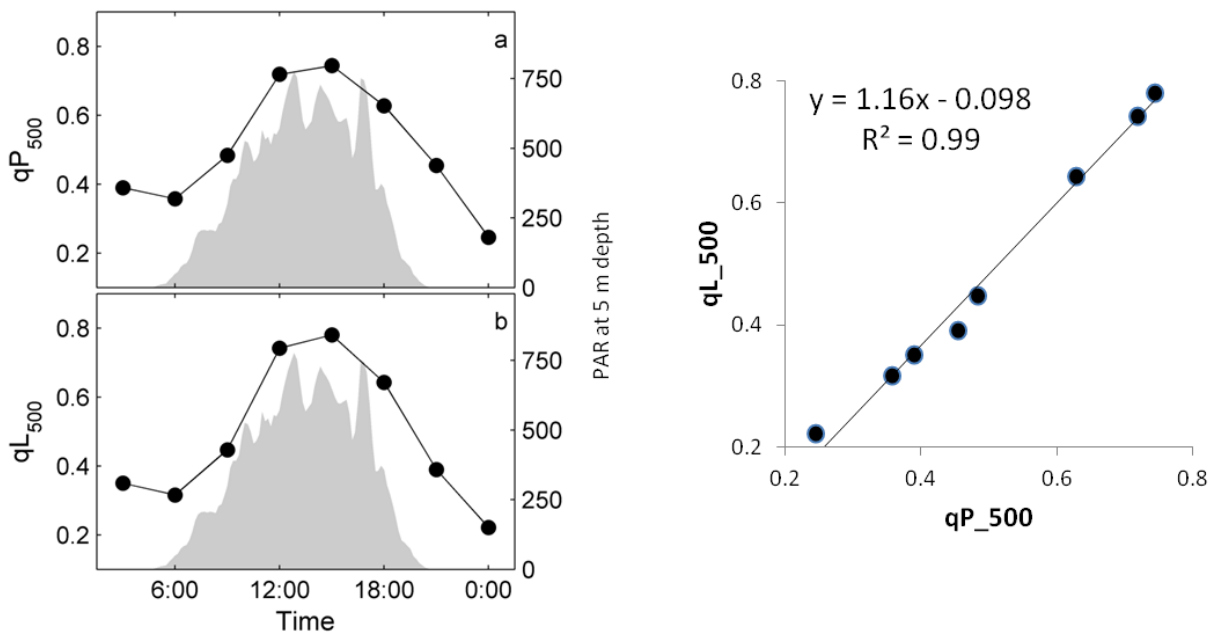
(16818 LN12) The low F_v/F_m values are entirely attributable to iron limitation? The question of blank subtraction raises its head here otherwise.

As discussed above, blank corrections were performed for each sample (page 7, lines 181-182).

(16818 LN18) Why introduce the term “qP” here (when F_q/F_v' is used earlier); also, why qP and not some other measure of the degree of RCII closure (see Oxborough et al. 2012)

The original manuscript actually described the term qP in the method section (page 16811, line 20), where we explicitly state that $F_q'/F_v' = qP$. We reasoned that using both, F_q'/F_v' and qP, while stating that they are the same, would give the reader the ability to see how the parameter is derive as well as making it easier to relate our findings to many earlier studies, which use qP. In the revised manuscript we use the term F_q'/F_v' throughout.

In response to the reviewers concern about different approaches to estimate the degree of RCII closure from ChlF yields, we below show two versions of Fig. 6d (Fig 5d in the revised manuscript).. The top panel shows the original figure, where the fraction of open RCII (i.e. the first stable electron acceptor Q_A oxidized) is estimated as F_q'/F_v' ($= qP$). This approach assumes zero energy transfer between closed and open RCII ('puddle' model). The bottom panel shows the same data, where the fraction of open RCII is estimated as $F_q'/F_v' \times F_o'/F'$ ($= qL$). This approach assumes perfect energy transfer between closed and open RCII ('lake' model).



As shown in the figures above, both approaches give very similar results, and lead to the exact same interpretation of the data.

(16818 LN28) I'm not sure the authors can robustly defend the statement "As the first study to investigate diurnal pattern of cellular energy allocation" – it's the first study to examine the empirical connection between ETR and 14C (net) uptake) but it does not look at cellular energy allocation!!!! Energy allocation is only subsequently 'inferred' through discussion/speculation via the patterns.

We agree with the reviewer and changed the wording of this section (page 16, lines 437-444).

(16822 LN10) – "In conclusion, we suggest that the observed changes in the conversion factor". OK, potential methodological artefacts aside (see points above, and as I said these need to be really robustly considered to ensure that the diel story holds), this entire section is a theoretical 'journey' with a laundry list of physiological pathways to explain how cells operate and therefore could possibly account for the diel decoupling.

I'm not sure the value this has without any real physiological evidence per se.

As such, I strongly recommend this entirely speculative section be toned down but also that 'caveat' text put in place upfront to state that this is purely speculative at this stage - possible diel coupling could be envisaged through increasing re-balancing of energy and/or reductant; for example. . .however, the nature and extent of operation of these various pathways and the exact nature with which diel coupling operates remains to be verified. This is important since depending on the environment or taxa under investigation one might imagine that these processes operate more strongly/weakly and hence ETR_{RCH} and 14C uptake more distantly/closely coupled.

We understand the reviewers concern and have rewritten the section to stress that our study does not include any direct verification of the cell physiological processes we suggest to be responsible for the observed decoupling between ETR_{RCH} and carbon fixation. We have also added a section about potential caveats, as suggest (page 19, lines 535-536).

(16823 LN17) – Blank issues again? Also, any evidence of chlororespiration (important under Fe limitation according to Behrenfeld and others) – this would be evident from the light response curves for Fq'/Fm' – this will also need to be discounted. Also, Suggett et al. (2009) MEPS notes that Fv/Fm can be as low as 0.35-0.4 for small flagellates under nutrient replete conditions – this will be the case where photoprotective pigments act to really drag Fv/Fm down. The bottom line is that there's a whole suite of variables that need to be discounted before Fe limitation alone is left as the smoking gun.

We did not mean to imply that iron limitation is the only reason for the low F_v/F_m . Rather; we wanted to give evidence for the iron-limited state of the phytoplankton assemblage sampled. We changed the wording of the section (page 20, lines 568-571).

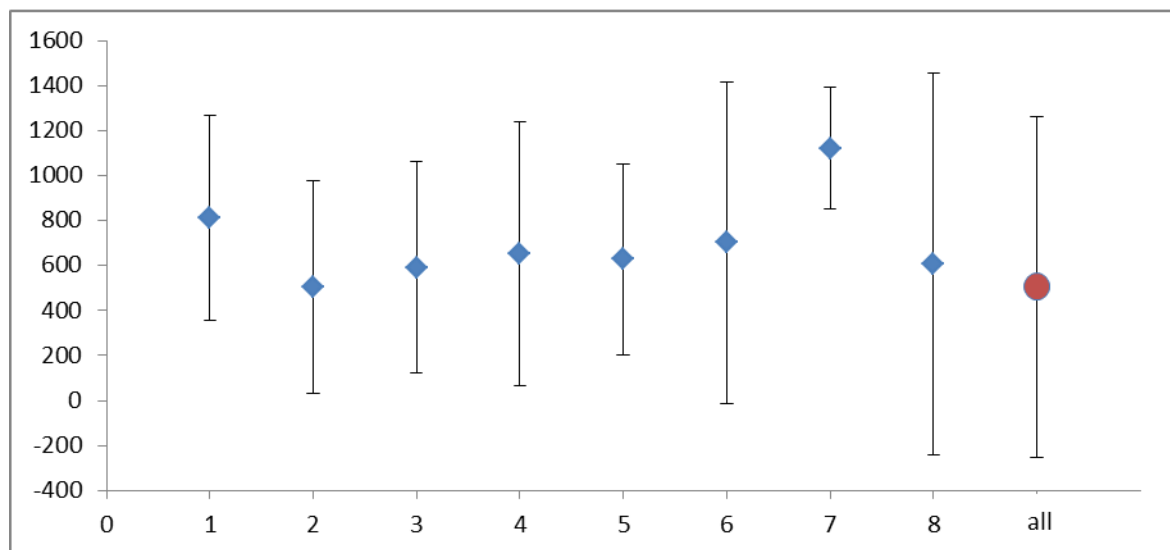
This aside, we can rule out the blank issue (as blanks correction was indeed performed), and chlororespiration should have been minimal as samples were incubated under low light before measurements.

(16824 LN22) – I liked Fig. 7 BUT there's an obvious (and necessary) analytical step missing – the coupling between the two variables appears to follow different trajectories for each different time bin; it would really help to run calculate (linear) regression slopes for each time point (and intercompare statistically these for the different time points).

This would objectively inform the authors if the coupling is drifting in a certain direction overtime and just whether time matters. By eye, a single linear regression for the whole data set would imply that diel variance is not important (i.e. the variance across the data set is too large to pull out any time differences) – the point being that time of day is clearly important BUT that NPQNSV can generally account for this? The authors allude to this in the discussion (16825 LN20) but this is not supported statistically and the reader has to take a large leap of faith.

The reviewer's suggestion is very good, and we show below the linear regression slopes and their standard errors of estimate (SEE) for each TP over the diurnal cycle. The figure shows that the slopes are, in fact, not statistically different from each other. We therefore removed the section where we discuss the differences in regression of different TP from the discussion, and replotted Fig 7 accordingly.

TP	1	2	3	4	5	6	7	8	all
time	3:00	6:00	9:00	12:00	15:00	18:00	21:00	0:00	
slope	811	505	593	653	628	701	1122	607	506
intercept	524	743	570	721	329	1199	378	1373	1887
SEE	457	471	470	586	423	714	273	849	758



More generally with this entire section, it reads as though the issue is done and dusted, i.e. NSV should “always” explain the relation between ETRCII and ^{14}C uptake (and hence that non-photochemical quenching always reflects how energy/reductant is utilised/rebalanced, according to the discussion by the authors, which it is unlikely to be – what about N-assimilation for example?); also, that at present the authors have only explored this approach for a single Fe limited region/community but would they expect it to hold for other taxa/communities where NPQ and physiological process differ and for different types of environmental limitation. Some word of caution are needed to tie back their findings to the (currently) limited scope of the data set.

In our original discussion, we discussed, at some length, a variety of limitations of this analysis. In response to the reviewer's comments, we have further revised the section to (hopefully) make it even clearer that our results present a novel and preliminary observation that requires significant follow up with future studies (page 1, line 31; page 22 lines 621-623; page 23, lines 649-652). We see the work as a first step, which requires validation before any broad conclusions can be reached.

Figure 3&4 – These figures could be combined – Ek could be added as a panel to figure 4 (as it stands I don't see that the Ek data alone warrants an independent figure when it could easily be included at the bottom of fig 3).

This is a good suggestion, and we have now combined these figures.

Figure 5 – I am not convinced about the need for the lines extrapolating between each timepoint – it only serves to visually fill in the gaps between samples (a lengthy 6 hours gap), which really should have been addressed at the time of sampling. The overall trend would still be apparent without this.

The lines have been removed.

Figure 6 – Tau should be included here, (after all, why not? – Fv/Fm and Sigma are here and I think Tau would provide an extra level of information in understanding how ETR and downstream processes (i.e. C-fixation) are linked

A panel showing $1/\tau$ has been included in Fig. 6.

Figure 7 – Whilst the overall correlation looks reasonably good, the different “trajectories” that seem to be apparent and need better consideration, see comment above.

See answer to comment above.

References

- Behrenfeld, M. J., Prasil, O., Babin, M. and Bruyant, F.: In search of a physiological basis for covariations in light-limited and light-saturated photosynthesis, *J. Phycol.*, 40(1), 4–25, 2004.
- Behrenfeld, M. J., Halsey, K. H. and Milligan, A. J.: Evolved physiological responses of phytoplankton to their integrated growth environment, *Philos. Trans. R. Soc. B Biol. Sci.*, 363(1504), 2687–2703, 2008.
- Gorbunov, M. Y., Kolber, Z. S., Lesser, M. P. and Falkowski, P. G.: Photosynthesis and photoprotection in symbiotic corals, *Limnol. Oceanogr.*, 75–85, 2001.
- Greg M. Silsbe, K. O.: Toward autonomous measurements of photosynthetic electron transport rates: An evaluation of active fluorescence-based measurements of photochemistry, *Limnol. Oceanogr. Methods*, 13(3), doi:10.1002/lom3.10014, 2015.
- Halsey, K. H. and Jones, B. M.: Phytoplankton Strategies for Photosynthetic Energy Allocation, *Annu. Rev. Mar. Sci.*, 7(1), 265–297, doi:10.1146/annurev-marine-010814-015813, 2015.

- Kolber, Z. and Falkowski, P. G.: Use of Active Fluorescence to Estimate Phytoplankton Photosynthesis in Situ, *Limnol. Oceanogr.*, 38(8), 1646–1665, doi:10.2307/2838443, 1993.
- Lawrenz, E., Silsbe, G., Capuzzo, E., Ylöstalo, P., Forster, R. M., Simis, S. G. H., Prášil, O., Kromkamp, J. C., Hickman, A. E., Moore, C. M., Forget, M.-H., Geider, R. J. and Suggett, D. J.: Predicting the Electron Requirement for Carbon Fixation in Seas and Oceans, *PLoS ONE*, 8(3), e58137, doi:10.1371/journal.pone.0058137, 2013.
- Laws, E. A.: Photosynthetic quotients, new production and net community production in the open ocean, *Deep Sea Res. Part Oceanogr. Res. Pap.*, 38(1), 143–167, 1991.
- Myers, J.: On the Algae: Thoughts about Physiology and Measurements of Efficiency, in *Primary Productivity in the Sea*, edited by P. G. Falkowski, pp. 1–16, Springer US. [online] Available from: http://link.springer.com/chapter/10.1007/978-1-4684-3890-1_1 (Accessed 28 August 2015), 1980.
- Niyogi, K. K.: Safety valves for photosynthesis, *Curr. Opin. Plant Biol.*, 3(6), 455–460, doi:10.1016/S1369-5266(00)00113-8, 2000.
- Oxborough, K., Moore, C. M., Suggett, D. J., Lawson, T., Chan, H. G. and Geider, R. J.: Direct estimation of functional PSII reaction center concentration and PSII electron flux on a volume basis: a new approach to the analysis of Fast Repetition Rate fluorometry (FRRf) data, *Limnol Ocean. Methods*, 10, 142–154, 2012.
- Robinson, C., Suggett, D. J., Cherukuru, N., Ralph, P. J. and Doblin, M. A.: Performance of Fast Repetition Rate fluorometry based estimates of primary productivity in coastal waters, *J. Mar. Syst.*, 139, 299–310, doi:10.1016/j.jmarsys.2014.07.016, 2014.
- Schuback, N., Schallenberg, C., Duckham, C., Maldonado, M. T. and Tortell, P. D.: Interacting Effects of Light and Iron Availability on the Coupling of Photosynthetic Electron Transport and CO₂-Assimilation in Marine Phytoplankton, *PLoS ONE*, 10(7), e0133235, doi:10.1371/journal.pone.0133235, 2015.
- Suggett, D. J., Moore, C. M. and Geider, R. J.: Estimating aquatic productivity from active fluorescence measurements, *Chlorophyll Fluoresc. Aquat.Sci. Methods Appl.*, 103–127, 2010.
- Vassiliev, I. R., Kolber, Z., Wyman, K. D., Mauzerall, D., Shukla, V. K. and Falkowski, P. G.: Effects of Iron Limitation on Photosystem II Composition and Light Utilization in *Dunaliellatertiolecta*, *Plant Physiol.*, 109(3), 963–972, doi:10.1104/pp.109.3.963, 1995.

Response to Anonymous Referee #2

We thank the reviewer for their comments and suggestions. Accompanying this response letter we provide a revised manuscript, in which we incorporated the reviewers suggestions, as

outlined below. In the revised manuscript, suggested changes from the original manuscript are written in blue font. The page and line numbers provided in our answers below refer to the revised manuscript.

General comments

The present paper examines the empirical relationships between carbon fixation and electron transfer measured by fast repetition rate fluorometry (FRRF) and their dependency on diel changes in solar irradiance under low iron availability.

To largest drawback of the FRRF techniques remaining to this day is the conversion of electron transfer to carbon fixation. This has been the focus of multiple recent studies. New algorithms for the direct derivation of reaction centre 2 concentrations from chlorophyll fluorescence measurements (Oxborough et al. 2012) enabled researchers, for the first time since the introduction of the technique, to measure electron transfer in absolute terms. Any conversion of electron transfer to carbon fixation, however, requires that these new algorithms and subsequent conversion factors hold under varying light conditions and nutrient availability. Whether this is actually the case has never been rigorously tested, and thus, the new RCII algorithm should probably be used with a certain degree of caution. A RCII-independent approach may, hence, be an alternative to the present approach that should be included in future work and warrants further in-depth studying. I, therefore, consider the present publication a valuable contribution for the field of fluorescence-based primary productivity measurements.

Specific comments

16805 L7/8 – “more recently” – Kolber & Falkowski 1993 is not exactly recent. Furthermore, Kolber et al. (1998) should probably be mentioned here as well, perhaps in favour of Schreiber’s work because the latter deals with multiple rather than single turnover techniques.

We were trying to convey the fact that active chlorophyll a fluorescence based methods (both single and multiple turnover techniques) are recent in relation to “traditional” incubation based methods including 14C-uptake studies. We have changed “more recently” to “Over the past two decades” (page 2, line 39).

16805 L 20-23 – Using a combination of $\Phi_d'e,C$ and $1/nPSII$ as a conversion factor is rather new to most people working with FRRF. Frankly, I still have somewhat of a hard time getting my head around this conversion factor with regards to its units and absolute values. To ease the reader into this, could the authors perhaps mention the previous approach of using $\Phi_d'e,C$ alone, emphasize why the new conversion factor is chosen over $\Phi_d'e,C$ and what one would expect as theoretical values, similar to the theoretical minimum of $\Phi_d'e,C$ of 4-5 mol e⁻ (mol C)⁻¹.

We agree with the reviewer and have added the suggested details to the revised manuscript (page 11, lines 284-287). A discussion about theoretical values of our conversion factor can be found in the original manuscript (page 16820, lines 19-23), and the revised version

on (page 18, lines 490-497).

16806 L5-8 References mentioned here did not study the mechanistic underpinning of the uncoupling between ETR and C fixation, but rather the empirical relationships between ETR and Carbon fixation. Either include references that focus on the underlying mechanisms or rephrase the sentence.

The sentence has been rephrased and now reads:

“For example, energy and reducing power (ATP and NADPH) from the photosynthetic light reaction can be used directly for the reduction or assimilation of limiting nutrients rather than for carbon fixation (e.g. Laws, 1991; Myers, 1980), resulting in an increased derived conversion factor K_c/n_{PSII} (e.g. Napoléon et al., 2013).”(page 3, lines 59-62).

16808 L6 – Unfortunate gap in the irradiance data! Could you perhaps just specify when the malfunction occurred and over which times you had to fill the data gap?

The time period for which the PAR data was extrapolated (bases on continuously logged SW radiation data from the NOAA buoy) was 14:00 – 17:00. This has been clarified in the revised manuscript (page 5, line 114).

16810 L 22: Are the four wavelengths of the Soliense FRRF exciting fluorescence one after another or are they used simultaneously?
Please clarify because other (mostly multiple turnover) fluorometers do not allow the user to combine multiple excitation wavelengths at once (instead one has to use them one after another).

The four excitation wavelength in the Soliense FRRF can be triggered separately or in combination, making it a truly versatile instrument. Data presented in the present study was acquired triggering all four wavelengths simultaneously. This has now been clarified in the current manuscript (page 7, line 188).

16811 – Equation 3 is missing the $\Delta d'PSII$ term. $\Delta d'PSII = 1 \text{ mol electrons (mol quanta)}^{-1}$, and is needed to end up with units of electrons and cancel out the mol quanta. It is often omitted in the literature because it takes a constant value of 1, however, it should be included.

This has been changed in the revised manuscript (page 8, line 212-214).

Also, this whole paragraph on FRR fluorometry makes no mention of a blank measurement. However, the blanks may be very important, especially in waters with low phytoplankton biomass. Please clarify whether blank measurements were carried out and how data were treated for blank correction.

Blank corrections were performed for each sample and values for each wavelength

automatically subtracted during the sample run. We added a description of the exact procedure for blank-correction in the revised methods section (page 7, line 181-182).

16812 L 4 – The SI unit for radioactivity is Becquerel (Bq), not Curie. Please convert accordingly.

This has been changed in the revised manuscript (page 9, line 234).

16812 L17 – 10 mL instead of “Ten”.

We spelled out this numbers at the beginning of sentences to be consistent with the editorial style of the journal.

16813 L 18-25. The authors may not yet be aware of an improved technique to fit ETR vs. E curves, which was introduced by Silsbe & Kromkamp (2012). One of the assumptions of a regression analysis is that the y-values are independent of the x-values. With irradiance (E) being a factor in the ETR equation (e.g. Eq. 3), this assumption does not hold. Silsbe and Kromkamp addressed this issue in their 2012 paper in L&O methods (Modeling the irradiance dependency of the quantum efficiency of photosynthesis. *Limnol. Oceanogr. Methods* 10, 645–652). Their approach also reduces the error of the fit at high irradiances (where quantum efficiency values become highly variable due to low variable fluorescence at high light). It may not make much of a difference in the derived P vs. E parameters, but this is certainly something to keep in mind for future work.

We strongly agree with the approach outlined in (Silsbe and Kromkamp, 2012), and will try to implement it in future studies. However, as the reviewer points out, and as is clear from the data presented in Silsbe and Kromkamp (2012), the different approach only marginally changes the derived fit parameters, with the largest effect on the error of the derived fit parameters (P_{max} and α). In particular, the derived error for α is likely to decrease, while the error of the fit parameter P_{max} is likely to increase since the parameters used to calculate ETR (σ , in particular) can be measured with much higher accuracy at low relative to high light. During the present study, errors of derived parameters were not large enough to obscure the diurnal patterns we observed. Thus the alternative fitting approach would not have an appreciable influence on our interpretation of our data.

16814 L 10-14 – The authors expect the new RCII algorithm of Oxborough et al. 2012 to not hold under Fe limiting conditions. Could you perhaps elaborate why? As far as I know, the algorithm has never been put to test under low Fe (or any other form of nutrient stress). This needs clarification.

This issue has also been addressed (at length) by reviewer #1. Below we repeat our answer as well as some data analysis, giving evidence that the approach does indeed not work when contrasting iron limited and iron replete conditions. We have changed the wording in the

methods section of the revised manuscript, to be less ambiguous about why the Oxborough approach was not applied in the present study. Additionally, in response to an insightful suggestion by reviewer #3, the revised manuscript now includes estimates of relative diurnal changes in $1/n_{PSII}$ (page 11, lines 292-315; page 14, lines 380-390; page 17, lines 487-488; page 18, lines 494-497).

The inherent assumption to the approach of Oxborough et al. is that the ratio of the rate constants of photochemistry (k_p) and fluorescence (k_f) stay within a narrow range. This is not the case under iron limitation, where k_p decreases while k_f increases (e.g. Vassiliev et al., 1995). Indeed, the original paper by Oxborough et al. cautioned that the approach relied on assumptions which might not hold under nutrient limitation, especially if the limiting nutrient is iron (Oxborough et al., 2012). This potential caveat was recently repeated by Robinson et al., 2014, who say:

“The calculation of [RCII] using the relationship between the minimum fluorescence parameter (F_o) and [RCII] as determined by Oxborough et al. (2012) may be sensitive to nutrient stress (C.M. Moore pers. comm.) which results in the enhanced uncoupling of chlorophyll complexes and PSII reaction centres (...).”

A recent publication by Silsbe et al. (2015) does include data for cultures grown without added iron, though no specific information is presented on the extent of iron limitation in these cultures. In the assessment of their data, Silsbe et al. note that:

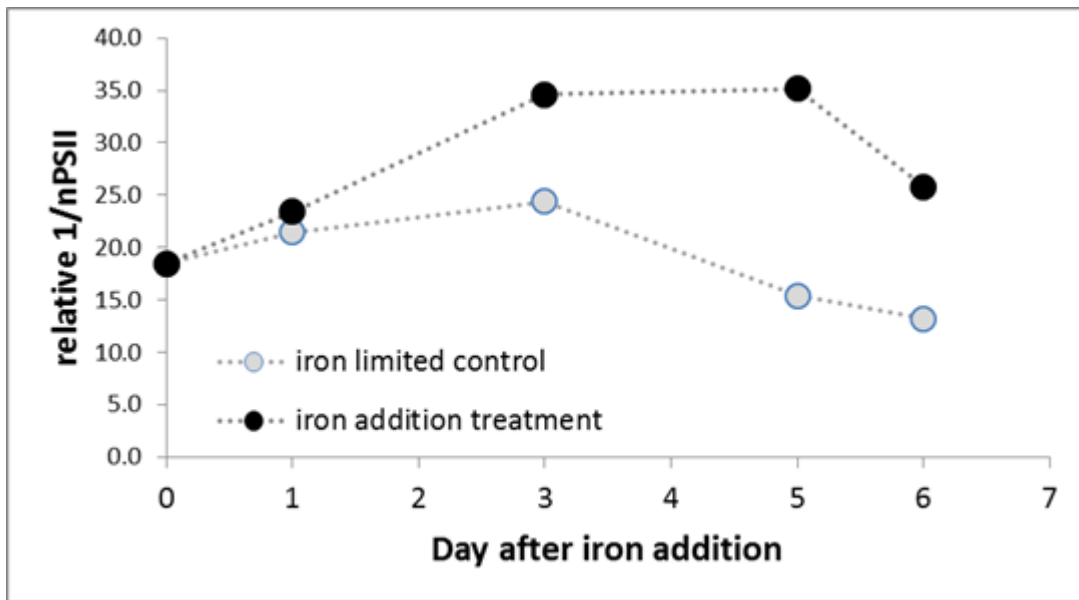
“...both Tp-Fe and Tw-Fe cultures grown in the absence of iron predicted higher [RCII] than measured. Consequently these cultures yielded lower K_R values than other cultures. This key finding is consistent with the concept that iron limited phytoplankton may accumulate a store of non-energetically coupled chlorophyll-binding complexes that increases the quantum yield of fluorescence (Φ_f) relative to iron replete phytoplankton (Behrenfeld and Milligan 2013; Macey et al. 2014). As K_R is proportional to Φ_P/Φ_f , an increase in Φ_f would diminish K_R as observed in this study. Omission of these iron-deplete cultures generally increased the mean K_R value for each instrument and reduced its variance...”

In order to further verify this evidence from the literature, we applied the Oxborough approach to our own data. The data shown below is from an on-board iron addition experiment conducted in the iron-limited NE subarctic Pacific, published in Schuback et al. (2015).

Below, we use values of F_o and σ_{PSII} in the dark-regulated state to derive information on the variability of $1/n_{PSII}$ during our iron-addition experiment (all values are mean of 3 biological replicates). Lacking the instrument specific calibration factor K_R , we were not able to derive absolute values for [RCII], but, since K_R is a constant, changes in F_o/σ_{PSII} should represent relative changes in [RCII]. Normalized to [chl a] we should be able to derive relative changes in

$1/n_{PSII}$. The data below show that $1/n_{PSII}$ increased after iron-addition, which is in contrast to numerous previously published studies showing increased $1/n_{PSII}$ (chl_a RCII¹) in iron limited cells (e.g. Macey et al., 2014; Vassiliev et al., 1995). Similarly, in our laboratory experiment, cultures well acclimated iron-limitation had a significantly lower relative $1/n_{PSII}$ than the iron replete cultures.

Day	Fe limited CONTROL					Fe ADDITION				
	sig	F0	relative [RCII]	[chl _a]	relative 1/n_PSII	sig	F0	relative [RCII]	[chl _a]	relative 1/n_PSII
0	963	26	0.03	0.50	18.4	963	26	0.03	0.50	18.4
1	906	25	0.03	0.60	21.5	841	26	0.03	0.72	23.4
3	981	49	0.05	1.22	24.4	743	46	0.06	2.12	34.6
5	910	111	0.12	1.88	15.4	821	182	0.22	7.79	35.1
6	920	121	0.13	1.73	13.2	819	302	0.37	9.49	25.8



16815 L14 – Could the authors please specify how they define the photic zone, i.e. as the 1% or 0.1% light level because different groups of researchers define it differently, and photosynthesis may take place well below the 1% light level (Kirk 1994)

The photic zone was defined as the 0.1% light level, which has been clarified in the revised version of the manuscript (page 12, line 326).

16816 L 6-27 and conversion factors presented in Fig. 1 and 2 – Why do the conversion factors differ so much between the two figures (2000-8000 e- RCII-1/C Chla-1 in Fig. 1, but only 2-10 e- RCII-1 C Chla-1 in Fig. 2)? If one divides the ETR_{max} by P_{max} for carbon fixation (or the corresponding alpha values by one another), one should end up with values of a few thousand e-

RCII-1/C Chla-1. Please clarify/fix accordingly.

16817 – Fig. 4 shows conversion factors of 2-12 x10⁴. This is what the axes in Fig. 3 should probably read as well?

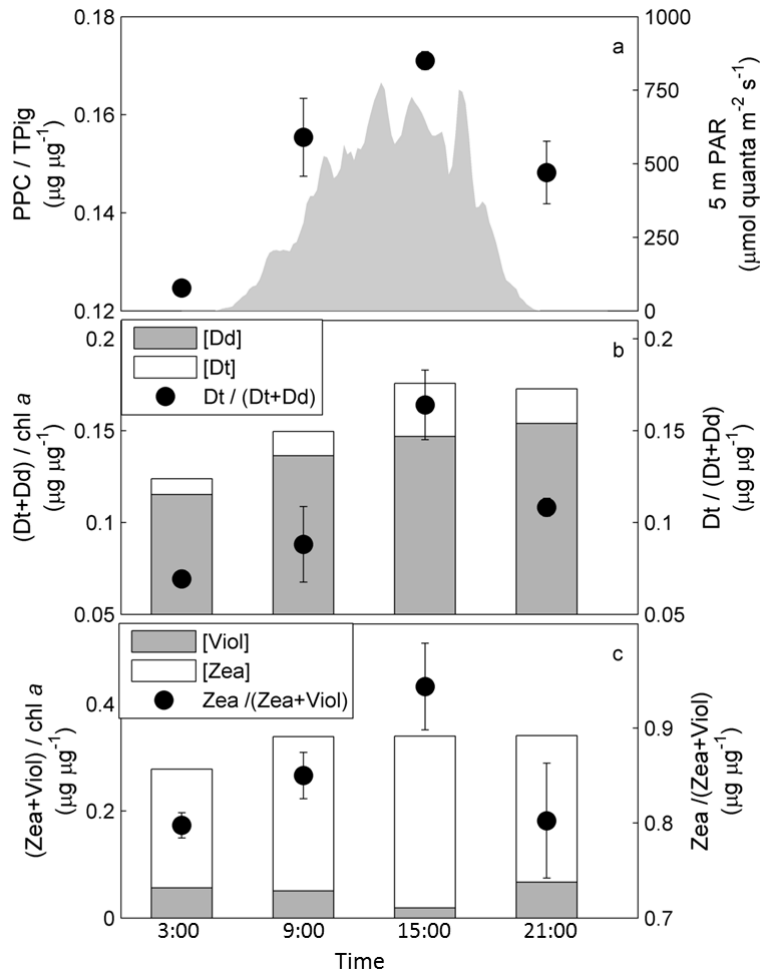
We thank the reviewer for pointing out this mistake and have corrected axes labels on Fig. 2 accordingly.

16817 – The in-text reference to Table 2 is misleading. Table 2 defines PPC, PSC etc. but does not actually present pigment ratios as suggested in the text. I would suggest mentioning this table in the methods and explain how the PPC and PSC were defined there.

We agree and have corrected the revised manuscript according to the reviewers' suggestions (page 6, lines 144-145).

16817 L18-29 – The calculated DES ratios account only for taxa containing a xanthophyll cycle based on diadinoxanthin and diatoxanthin but not for taxa containing a violaxanthin zeaxanthin-based xanthophyll cycle (chlorophytes and prasinophytes). According to the Chemtax results, diadinoxanthin-diatoxanthin containing taxa account for 35 % of the total chlorophyll in the phytoplankton community, chlorophytes and prasinophytes for 28%. Could the authors perhaps also calculate the DES ratios for the “green” group or otherwise explain why they have been left out?

The violaxanthin zeaxanthin- based xanthophyll cycle shows the same trend as the diadinoxanthin-diatoxanthin based xanthophyll cycle. We have incorporated these data into a revised version of Fig 4, as shown below.



Also note that accurate DES calculation requires quick sampling due to rapid epoxidation of the diatoxanthin back to diadinoxanthin (and zeaxanthin to violaxanthin). For such purposes, samples are usually flash-frozen in liquid N₂ within 1-2 minutes after their removal from the light source.

Given that sampling with Niskin bottles on a rosette and subsequent filtration probably takes on the order of 30 min (?), the ratios presented here may be off. Perhaps the authors could just acknowledge that with one line.

The samples were taken from the underway sampling system of the ship, and HPLC samples were always given priority during the filtration procedure. However, the reviewer's concerns are valid, and we have acknowledged this potential caveat in the revised manuscript (page 14, lines 410-412). Great care was taken to use dark bottles and low light during the filtration procedure. Therefore, it is likely that the observed diurnal trend in DES ratio would have been even larger, if we would have been able to filter samples faster. This would have further confirmed our conclusion that the sampled phytoplankton assemblage experienced, and reacted to, super-saturating light intensities for part of the day.

Also, please note the typo on line 28: de-epoxidation, not de-epoxilation.

Corrected.

16818 L15 – “Fv/Fm (. . .) half of the values expected from nutrient DEplete phytoplankton.” Is this correct or should this read half the values expected from nutrient REplete phytoplankton?

We thank the reviewer for pointing out this mistake, which has been corrected in the revised manuscript.

16820 L22, 23 Superscript ‘-1’ is missing in mol e- mol C-1.

Corrected.

168221 L28- 16822 L14 – It is intriguing to conclude that the observed effects on the conversion factor and optical properties are the result of iron limitation. This, to me, seems rather speculative because we do not have a comparison with iron replete conditions, which would need further field or culture work. I understand that this would be beyond the scope of this paper, but perhaps the authors could acknowledge that and insert a “disclaimer” highlighting possible future work to resolve this issue.

The paragraph references our previous study (Schuback et al., 2015), which compares iron deplete and replete field samples as well as laboratory cultures. We rephrased the section to further emphasise this.

16823 L17-29 – Please note that Fv/Fm also shows considerable taxonomic variability / dependency (Suggett et al. 2009 – MEPS Vol. 376:1-19).

Based on the Chemtax results, community composition did not changed throughout the day and, hence, taxonomic dependency of Fv/Fm is probably negligible. Perhaps the authors could acknowledge that with a brief statement.

The section has been rewritten accordingly (page 20 lines 563-565).

16824 L22 and Fig. 7 -Please note that correlation and regression are not the same methods and the two terms should not be used interchangeably (e.g. Field 2006 – Discovering Statistics using SPSS, 2nd edition, Sage Publishing. If the authors aim to establish mathematical relationships between NPQ and the conversion factor (and calculate slopes), then they should use a regression. An appropriate description should also be included in the methods. I am also not convinced that one may not miss some essential information by lumping all the data together into one regression. I looks like the slopes of the regression lines may vary with time of day if the data set was broken up according to the different sampling times. Furthermore, for some sampling time points, the relationship between NPQ and the conversion factor seems to have somewhat of a curvature (e.g. 3:00, 6:00).

The entire section has been rewritten; please see also responses to reviewer #1. We have now more explicitly examined the time-dependence of the correlation and not found any statistically significant trends.

References

- Laws, E. A.: Photosynthetic quotients, new production and net community production in the open ocean, *Deep Sea Res. Part Oceanogr. Res. Pap.*, 38(1), 143–167, 1991.
- Macey, A. I., Ryan-Keogh, T., Richier, S., Moore, C. M. and Bibby, T. S.: Photosynthetic protein stoichiometry and photophysiology in the high latitude North Atlantic, *Limnol. Oceanogr.*, 59(6), 1853–1864, doi:10.4319/lo.2014.59.6.1853, 2014.
- Myers, J.: On the Algae: Thoughts about Physiology and Measurements of Efficiency, in *Primary Productivity in the Sea*, edited by P. G. Falkowski, pp. 1–16, Springer US. [online] Available from: http://link.springer.com/chapter/10.1007/978-1-4684-3890-1_1 (Accessed 28 August 2015), 1980.
- Oxborough, K., Moore, C. M., Suggett, D. J., Lawson, T., Chan, H. G. and Geider, R. J.: Direct estimation of functional PSII reaction center concentration and PSII electron flux on a volume basis: a new approach to the analysis of Fast Repetition Rate fluorometry (FRRf) data, *Limnol Ocean. Methods*, 10, 142–154, 2012.
- Robinson, C., Suggett, D. J., Cherukuru, N., Ralph, P. J. and Doblin, M. A.: Performance of Fast Repetition Rate fluorometry based estimates of primary productivity in coastal waters, *J. Mar. Syst.*, 139, 299–310, doi:10.1016/j.jmarsys.2014.07.016, 2014.
- Schuback, N., Schallenberg, C., Duckham, C., Maldonado, M. T. and Tortell, P. D.: Interacting Effects of Light and Iron Availability on the Coupling of Photosynthetic Electron Transport and CO₂-Assimilation in Marine Phytoplankton, *PLoS ONE*, 10(7), e0133235, doi:10.1371/journal.pone.0133235, 2015.
- Silsbe, G. M. and Kromkamp, J. C.: Modeling the irradiance dependency of the quantum efficiency of photosynthesis, *Limnol. Oceanogr. Methods*, 10(9), 645–652, doi:10.4319/lom.2012.10.645, 2012.
- Silsbe, G.M. et al.: Toward autonomous measurements of photosynthetic electron transport rates: An evaluation of active fluorescence-based measurements of photochemistry, *Limnol. Oceanogr. Methods*, 13(3), doi:10.1002/lom3.10014, 2015.
- Vassiliev, I. R., Kolber, Z., Wyman, K. D., Mauzerall, D., Shukla, V. K. and Falkowski, P. G.: Effects of Iron Limitation on Photosystem II Composition and Light Utilization in *Dunaliella tertiolecta*, *Plant Physiol.*, 109(3), 963–972, doi:10.1104/pp.109.3.963, 1995.

Response to Anonymous Referee #3

We thank the reviewer for their very insightful comments and ideas. Following their suggestions we have added substantial additional analysis of our data. This response letter is accompanied by a revised manuscript, which allows to see how we suggest to incorporate these changes into the original narrative. In the revised manuscript, parts which differ from the original discussion paper are written in blue font. All page and line numbers we give in our answers below refer to the revised manuscript.

General Comments

This study examines diel periodicity of photosynthetic electron transport and carbon fixation in iron-limited waters of the subarctic Pacific Ocean. A comparison of active fluorescence light-response curves and ^{14}C -irradiance curves reveal the stoichiometry between reaction center II (RCII)-specific electron transport rates and carbon fixation rates vary by a factor of 3.5 throughout the day. This diurnal variability confounds the accuracy in which active fluorescence measurements can be scaled into more ecologically relevant carbon fixation rates. The authors provide a robust review of the myriad of non-carbon fixation pathways that consume photosynthetic energy (ATP and reductant), and suggest that endogenous periodicity in these pathways likely cause some of the observed decoupling. The authors also present an empirical relationship demonstrating that non-photochemical quenching (NPQ) explains a significant fraction of the decoupling between RCII-specific electron transport and carbon fixation rates. This study provides a clear demonstration of disparate diurnal variations in RCII specific electron transport and carbon fixation rates. While this lack of co-variation isn't surprising given our understanding of circadian patterns in phytoplankton physiology (e.g. Behrenfeld et al. 2008), this manuscript nevertheless is a useful contribution to the literature. My largest criticism of this manuscript is that the authors cannot address whether this variability is driven by diurnal changes in the electron requirement of carbon fixation (Phie,C) or the number of functional reaction centers normalized to chlorophyll a (nPSII). In fact we know that nPSII decreases in high light (Behrenfeld et al. 2002), and this is generally consistent with the highest $\text{Phie,C} \times 1/\text{nPSII}$ occurring midday (Fig 2A). Given that a properly calibrated active fluorometer can now estimate nPSII through an instrument specific conversion factor (KR, Oxborough et al. 2012 L&O Methods; Silsbe et al. 2015 L&O Methods), I feel as though the authors have missed an opportunity to more significantly advance the literature.

The authors mention that they did not attempt the new nPSII protocol as it is likely invalid for iron-limited phytoplankton. This is likely true because iron-limited phytoplankton can possess surplus photosynthetic antennae that are decoupled from photosynthetic reaction centers (Schrader et al 2009 PLoSOne). As the new nPSII protocol varies from first principles with F_0 , decoupled antennae increase F_0 independent of nPSII. That said I would be surprised if this overestimation of nPSII has a diel pattern, in other words surplus antennae remain uncoupled from photosynthetic reaction centers over the course of the day so long as iron-limitation

remains. If the authors can estimate n_{PSII} from F_0 , then this study could better elucidate the diurnal periodicity of $\Phi_{e,C}$ alone. If the authors do not have access to an oxygen flash yield system that is required to derive K_R to estimate n_{PSII} (Oxborough et al. 2012), then I suggest estimating K_R using a chlorophyll a standard following Silsbe et al. (2015). Many newer active fluorescence studies implement this approach (e.g. Robinson et al. 2014, J. Mar. Sys), and if the authors can make these changes it would likely increase this manuscript's impact.

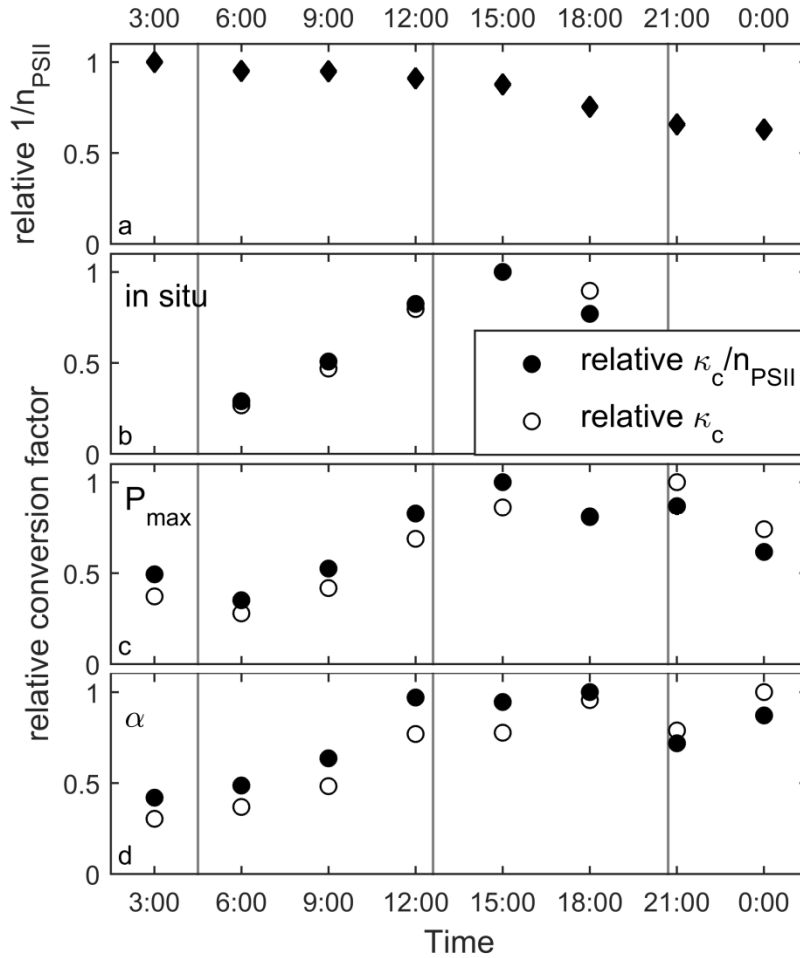
As the reviewer explains correctly, the Oxborough approach to estimate absolute values of [RCII] was not applied in the original manuscript because the inherent assumption that the ratio of the rate constants of photochemistry (k_p) and fluorescence (k_f) stay within a narrow range, does not hold under iron limitation, where k_p decreases while k_f increases (e.g. Vassiliev et al., 1995) (see also answers to reviewers #1 and #2). As the reviewer points out, the increase in k_f under iron limitation is likely caused by energetically decoupled light harvesting complexes (DLHCs) (Behrenfeld and Milligan, 2013; Schrader et al., 2011), and we have added this information to the revised manuscript (page 11, line 295-303).

As shown clearly in response to reviewer #2, it is not possible to apply the Oxborough approach when comparing data from contrasting levels of iron limitation. However, it can indeed be argued that the phytoplankton assemblage sampled experienced a constant degree of iron limitation during the present study. Therefore, it is likely that the amount of DLHCs remained constant, which could result in a constant (albeit much lower) k_p/k_f . While this is speculation, and we do not have any experimental data on diurnal behaviour of DLHCs, we do agree with the reviewer's reasoning.

The reviewer suggests estimating K_R using a chlorophyll standard, as has been done in Silsbe et al.(2015), who show that a K_R value estimated in this way agrees relatively well with a K_R value derived the 'traditional' way, for six instruments tested. However, the same study also points out that for cultures grown without added Fe (no additional information on the actual degree of Fe limitation is given) the Oxborough approach (applying this K_R value) predicted higher [RCII] than was measured using oxygen flash yields. Therefore, we do not think it is possible to obtain an instrument specific K_R value which will result in accurate absolute values of [RCII] using a chlorophyll standard, if the phytoplankton assemblage sampled was iron limited.

Lacking the instrument specific calibration factor K_R , we were not able to derive absolute values for [RCII] (and in turn $1/n_{PSII}$). However, since K_R can be assumed constant (as long as the degree of iron limitation does not change), changes in of F_0/σ_{PSII} should represent relative changes in [RCII]. We should thus be able to derive relative changes in $1/n_{PSII}$, as suggested by the reviewer.

Below, we show how we applied this simplified version of the Oxborough approach to calculate relative diurnal changes in $1/n_{PSII}$ which, in turn, were used to deduce relative diurnal changes in $\Phi_{e,C}$ (K_c).



Here, we calculated relative values of $1/n_{PSII}$ for each TP as $(F_o/\sigma_{PSII})/[chl\ a]$, and scaled the values to 1 (panel a). Relative values of $1/n_{PSII}$ calculated in this way are highest at pre-dawn, stay relatively constant until the afternoon, and decrease by 37% from the first to the last TP. By comparison, the lumped conversion factor K_c/n_{PSII} changes by 245% for in situ irradiances (panel b), 185% at light saturation (P_{max} ; panel c) and 138% at light limitation (alpha; panel d).

We used the relative values of $1/n_{PSII}$ shown in panel (a) to deduce relative changes in K_c from the lumped conversion factor. The filled symbols in panel (b)-(c) are values of the conversion factor K_c/n_{PSII} , as shown in Fig. 2 and Fig. 3 of the original manuscript, scaled to 1. The open symbols are relative values of K_c derived by dividing the relative values of K_c/n_{PSII} by $1/n_{PSII}$. These derived values show that the diurnal change in relative K_c/n_{PSII} are very similar to diurnal changes in relative K_c , suggesting that variability in K_c drives most of the variability in the lumped conversion factor. The above figure and analysis are now included in the manuscript (page 11, lines 292-315; page 14, lines 380-390; page 17, lines 487-488; page 18, lines 494-497)

16805 – 20. Some references for the plasticity in pH_{le,C} and nPSII are needed. As active fluorometers can be calibrated to estimate nPSII, mentioning this technique (Oxborough et al. 2012, Silsbe et al. 2015) is warranted in this paragraph.

We have added range of variability encountered as 1.15 – 54.2 mol e⁻ mol C⁻¹ for K_c (Lawrenz et al., 2013) and approx. 200 – 950 mol chl_a mol RCII⁻¹ for 1/n_{PSII} (Suggett et al., 2010) to the revised manuscript (page 11, lines 284-287).

Furthermore, we revised the entire manuscript to better acknowledge the Oxborough approach for estimating absolute values of [RCII] directly from FRRF measurements. We also discuss why the approach has limitations under conditions of iron limitation, and how we apply a simplified version of it to our data to obtain relative [RCII] estimates.

16807 – 5. I would define NPQNSV as the ratio of the total non-photochemical dissipation in the light adapted state to the rate constant of photochemistry (McKew et al. 2013).

We added a sentence with this definition to the method section of the revised manuscript (page 9, lines 227-230).

16810 – 22. Are the LED lights at different wavelengths flashed in sequence or at the same time?

For all data shown in the present study, the four wavelengths were applied simultaneously. This is now clarified in the revised manuscript (page 7, lines 188).

16810 – Section 2.5. Was background (filtrate) fluorescence measured and subtracted from profile data?

Background fluorescence was measured and subtracted for each time point. We have added a sentence about this to the method section of the revised manuscript (page 7 lines 181-182).

16815 – 12. Please verify that daily incident irradiance was 53 236 Umol quanta m⁻²? This corresponds to a daily value of 0.053 mol quanta m⁻² d⁻¹, which seems a factor of 1000 too small (<http://oceancolor.gsfc.nasa.gov/cgi/l3>).

We thank the reviewer for pointing out this mistake. The daily incident irradiance was 31.94 mol quanta m⁻² d⁻¹, which is in agreement with values expected for this oceanic region and time of the year. The value has been corrected in the revised manuscript (page 12, line 326).

16821 – 3 to 27. This paragraph can be shortened, and you may want to look at Geider et al. (2009 Plant Ecology and Diversity) who tabulate the electron requirement of the dominant non-carbon fixation pathways.

The section has been shortened.

Figure 3: Combine with Figure 2 and reduce the range in the Y-axis.

The two figures have been combined (Fig. 2 in revised manuscript). However, we did not change the range of the Y-axis, as it is our intention to show E_k in relation to the available irradiance.

Figure 5 and 6: These figures should probably be combined.

In response to suggestions from reviewers #1 and #2 we added a panel to both Fig. 5 and Fig. 6 (Fig. 4 and Fig. 5 in revised manuscript). We feel that both figures now contain sufficient information to remain as separate figures, where Fig. 4 deals specifically with pigment ratios and Fig. 5 specifically with FRRF derived parameters only.

1 Diurnal Variation in the Coupling of Photosynthetic 2 Electron Transport and Carbon Fixation in iron-limited 3 Phytoplankton in the NE subarctic Pacific

4
5 N. Schuback¹, M. Flecken², M. T. Maldonado¹, P. D. Tortell^{1,3}

6 [1]{Department of Earth, Ocean and Atmospheric Sciences, University of British Columbia,
7 Vancouver, BC, Canada}

8 [2]{RWTH Aachen University, Aachen, Germany}

9 [3]{Department of Botany, University of British Columbia, Vancouver, BC, Canada}

10 Correspondence to: N. Schuback (nschuback@eos.ubc.ca)

11 12 Abstract

13 Active chlorophyll *a* fluorescence approaches, including fast repetition rate fluorometry
14 (FRRF), have the potential to provide estimates of phytoplankton primary productivity at
15 unprecedented spatial and temporal resolution. FRRF-derived productivity rates are based on
16 estimates of charge separation at PSII (ETR_{RCII}), which must be converted into ecologically
17 relevant units of carbon fixation. Understanding sources of variability in the coupling of ETR_{RCII}
18 and carbon fixation provides physiological insight into phytoplankton photosynthesis, and is
19 critical for the application of FRRF as a primary productivity measurement tool. In the present
20 study, we simultaneously measured phytoplankton carbon fixation and ETR_{RCII} in the iron-
21 limited NE subarctic Pacific, over the course of a diurnal cycle. We show that rates of ETR_{RCII}
22 are closely tied to the diurnal cycle in light availability, whereas rates of carbon fixation appear
23 to be influenced by endogenous changes in metabolic energy allocation under iron-limited
24 conditions. Unsynchronized diurnal oscillations of the two rates led to 3.5-fold changes in the
25 conversion factor coupling ETR_{RCII} and carbon fixation (K_c/n_{PSII}). Consequently, diurnal

26 variability in phytoplankton carbon fixation cannot be adequately captured with FRRF
27 approaches if a constant conversion factor is applied. Utilizing several auxiliary
28 photophysiological measurements, we observed that a high conversion factor is associated with
29 conditions of excess light, and correlates with the increased expression of non-photochemical
30 quenching (NPQ) in the pigment antenna, as derived from FRRF measurements. The observed
31 correlation between NPQ and K_c/n_{PSII} , which requires further validation, has the potential to
32 improve estimates of phytoplankton carbon fixation rates from FRRF measurements alone.

33 1 Introduction

34 Marine phytoplankton account for ~ 50% of global carbon fixation (Field et al., 1998), and
35 play a key role in Earth's biogeochemical cycles. Understanding the spatial and temporal patterns
36 in marine primary productivity and its response to environmental variability is thus a central
37 oceanographic research question. Traditionally, rates of phytoplankton primary production have
38 been measured using incubation-based assays, tracing the evolution of oxygen or the assimilation
39 of CO₂ (Williams et al., 2008). Over the past two decades, bio-optical approaches based on
40 measurements of active chlorophyll *a* fluorescence (ChlF) yields (Kolber and Falkowski, 1993;
41 Schreiber, 2004) have emerged as an attractive alternative, avoiding artifacts related to bottle
42 containment, and achieving unparalleled spatial and temporal resolution. The method most
43 prominently applied to measure ChlF yields in field assemblages of marine phytoplankton is fast
44 repetition rate fluorometry (FRRF) (Kolber et al., 1998). ChlF yields, as measured by FRRF, can
45 be used to estimate electron transport in photosystem II (ETR_{RCII} , mol e⁻ mol RCII⁻¹ s⁻¹), and
46 these rates can be converted to carbon units based on theoretical calculations. However,
47 empirical comparison of FRRF-derived ETR_{RCII} and carbon fixation data has shown that the
48 derived conversion factor varies significantly with changes in the physiology and taxonomic
49 composition of phytoplankton assemblages (Suggett et al., 2010; Lawrenz et al., 2013).

50 The conversion factor linking ETR_{RCII} and carbon fixation consists of two parameters, the
51 amount of chlorophyll *a* per number of functional PSII reaction centers ($1/n_{PSII}$; mol chl *a* mol
52 RCII⁻¹) and the electron requirement for carbon fixation (K_c ; mol e⁻ mol C⁻¹; note that in most
53 previous studies, this latter parameter has been denoted as $\Phi_{e:C}$). Plasticity in both $1/n_{PSII}$ and K_c

54 can be observed at the physiological and taxonomic level, and is ultimately a function of given
55 environmental conditions.

56 In order to optimize growth under fluctuating environmental conditions, phytoplankton
57 photosynthesis and downstream metabolic processes exhibit great plasticity and
58 interconnectivity, allowing rapid responds to changes in fluctuating light and nutrient levels. This
59 physiological regulation influences the coupling between ETR_{RCII} and carbon fixation. For
60 example, energy (ATP) and reducing power (NADPH) from the photosynthetic light reaction can
61 be used directly for the reduction or assimilation of limiting nutrients, rather than for carbon
62 fixation (e.g. Laws, 1991; Myers, 1980), resulting in an increased conversion factor K_c/n_{PSII} (e.g.
63 Napoléon et al., 2013). Furthermore, K_c/n_{PSII} has been shown to increase under excess light
64 conditions (Babin et al., 1996; Cheah et al., 2011; Corno et al., 2006; Fujiki et al., 2007; Goto et
65 al., 2008; Kaiblinger and Dokulil, 2006; Napoléon et al., 2013; Napoléon and Claquin, 2012;
66 Raateoja, 2004), when the rate of charge separation in RCII can outpace the rate of electron
67 transport along the photosynthetic electron transport chain (ETC). In order to alleviate the
68 ensuing “backpressure”, which can lead to e.g. singlet oxygen formation and photoinhibition,
69 photosynthetic organisms evolved a number of “safety valves” along the ETC (e.g. Niyogi,
70 2000). Activation of these alternative electron pathways increases the conversion factor K_c/n_{PSII} .
71 In a previous study, we showed that low iron concentrations enhanced the effect of excess light,
72 further increasing the conversion factor K_c/n_{PSII} (Schuback et al., 2015).

73 Given the well-established effect of excess light on the coupling of photosynthetic electron
74 transport and carbon fixation, it is likely that the two rates decouple over the course of a diurnal
75 cycle, if excess irradiance is encountered at noon. However, to our knowledge, there are no
76 direct experimental studies of the diurnal changes in the coupling of ETR_{RCII} and carbon fixation
77 in marine phytoplankton.

78 In the present study we simultaneously measured rates of ^{14}C -uptake and ETR_{RCII} in iron-
79 limited phytoplankton assemblages in the NE subarctic Pacific over the course of a 24 hour
80 diurnal cycle. Our results show that the conversion factor K_c/n_{PSII} , derived for in situ irradiances
81 at 5 m depth, varied significantly (by a factor of 3.4), with most of the variability attributable to
82 diurnal changes in K_c . Unless both carbon fixation and ETR_{RCII} are measured and integrated over
83 a whole diurnal cycle (e.g. Suggett et al., 2006), diurnal variability in K_c/n_{PSII} should be
84 considered, along with phytoplankton taxonomy and nutrient status (Lawrenz et al., 2013), when

85 deriving regional conversion factors between ETR_{RCII} and carbon fixation. Building on
86 previously published results (Schuback et al., 2015), we show that the magnitude and variability
87 of K_c/n_{PSII} can be correlated to FRRF-based measurements of non-photochemical quenching
88 (NPQ_{NSV}).

89 **2 Methods**

90 **2.1 Study site and water-column hydrography**

91 Field sampling was conducted on board the *CCGS John P. Tully* on June 17th/18th 2014. During
92 the sampling period, the research vessel stayed within close proximity (10 km) to Ocean Station
93 Papa (OSP), located in iron-limited waters of the NE subarctic Pacific (50 °N, 145 °W)
94 (<https://www.waterproperties.ca/linep/>). We acknowledge that our sampling approach is not truly
95 Lagrangian, and some variability in nutritional status and taxonomic composition of
96 phytoplankton assemblage could have occurred due to water mass advection. However, we
97 expect that surface hydrography and phytoplankton characteristics are sufficiently homogeneous
98 in this oceanic region, such that minor water mass advection would not have significantly
99 influenced primary productivity or photophysiological parameters measured over the diurnal
100 cycle.

101 During our occupation of OSP, we conducted five CTD casts (three casts during the 24 hour
102 diurnal experiment and one each before and after the diurnal sampling) to characterize variability
103 in temperature and salinity depth profiles, from which we derived seawater density using the
104 GSW toolbox in MATLAB (McDougall and Barker, 2011). Mixed layer depth (MLD) was
105 calculated from a density difference criterion ($\Delta\sigma = 0.05 \text{ kg m}^{-3}$). The depth profile of
106 photosynthetically available radiation (PAR, 400-700nm, $\mu\text{mol quantam}^{-2} \text{ s}^{-1}$) through the upper
107 100 m of the water column was obtained using a PAR sensor (Biospherical QSP-400) mounted
108 on the rosette during one of the CTD casts (12:30 local time (LT)). The optical extinction
109 coefficient, k_d (m^{-1}), was calculated as:

$$110 \quad k_d = (\ln E_0 - \ln E_z)/z \quad (1)$$

111 Where E_0 is surface irradiance and E_z is irradiance at depth z (m). Surface PAR (E_0^+) was
112 continuously logged (10 min intervals) with a LI-1000 down-welling PAR sensor (LI-COR,

113 USA), mounted in a non-shaded position on the ship's superstructure, at a height of ca 7 m above
114 the sea-surface. Unfortunately, 3 hours of PAR data (14:00-17:00 LT) were lost due to an
115 instrument malfunction. To fill the data gap, we utilized shortwave solar radiation data from a
116 nearby moored surface buoy, operated by the Ocean Climate Stations (OCS) group at Pacific
117 Marine Environmental Laboratory of the National Oceanic and Atmospheric Administration
118 (PMEL-NOAA). All mooring data are available from the NOAA OCS website
119 (<http://www.pmel.noaa.gov/OCS>). We aligned the two sets of irradiance data (ship-based and
120 surface mooring) and extrapolated over the 3 hour gap in order to obtain consistent E_0^+ for the
121 timespan of the diurnal experiment. Surface reflectance was calculated as a function of solar
122 zenith angle following Kirk (2011) using the R package 'phytotools' (Silsbe, 2015). Subtracting
123 surface reflectance provides PAR just under the air-ocean interface (E_0^-). PAR at 5 m depth
124 (E_{5m}^-) was calculated as $E_{5m}^- = E_0^- \exp(k_d \times 5m)$.

125 Macro-nutrients (P, N, Si) were measured on samples from 2 CTD-rosette casts following the
126 methods outlined in Barwell-Clarke (1996). Additional measurements of surface water (~ 5 m)
127 temperature and salinity were derived from the ship's thermosalinograph (TSG) connected to a
128 continuous seawater supply, and also from the NOAA mooring.

129 **2.2 Sample collection**

130 Seawater samples were collected from the seawater intake system (ca 5 m depth) every 3 hours
131 over a 24 hour period and processed immediately for a variety of physiological assays described
132 below. The resulting dataset consists of 8 time-points (TPs). Local sunrise, solar noon and sunset
133 were at 6:30, 14:40 and 22:50, respectively, resulting in 3 night-time TPs (3:00, 23:00, 0:00) and
134 5 day-time TPs (6:00, 9:00, 12:00, 15:00, 18:00). Samples taken at each TP are summarized in
135 Table 1.

136 **2.3 [chl a] and HPLC**

137 At each TP, duplicate 500 ml samples for [chl a] were filtered onto pre-combusted 25 mm glass
138 fiber filters (GF/F) using low vacuum pressure (<5 mm Hg), taking care to keep the filters out of
139 direct light. Filters were stored at -20 °C and analyzed following the method of Welschmeyer
140 (1994) within two weeks of collection. At 4 TPs (3:00, 9:00, 15:00, 21:00) duplicate 2.2 L
141 samples for pigment analysis were filtered onto pre-combusted 25 mm GF/F, as above. Filters

142 were blotted dry with absorbent paper, flash frozen in liquid nitrogen and stored at -80 °C until
143 analysis by reverse-phase high pressure liquid chromatography (HPLC) following the method of
144 (Pinckney, 2013). The identified pigments were grouped into photosynthetic carotenoids (PSC),
145 photoprotective carotenoids (PPC) and total chlorophyll (TChl) as outlined in Table 2. Ratios of
146 these pigment groups were used to assess diurnal changes in the extent of light stress
147 experienced by the whole phytoplankton assemblage. Xanthophyll cycling (XC) pigments of
148 chromophytes (diatoxanthin (Dt) and diadinoxanthin (Dd)) as well as xanthophyll cycling
149 pigments of prasinophytes and chlorophytes (violaxanthin (Viol) and zeaxanthin (Zea)) were
150 assessed with regard to their relative abundance ((Dt+Dd)/chl *a* and (Zea+Viol)/chl *a*), and de-
151 epoxidation state ratios (DES, Dt/(Dt+Dd) and Zea/(Zea+Viol)). Furthermore, pigment data were
152 used to estimate the relative abundance of different phytoplankton taxa at our sampling site.
153 CHEMTAX analysis was performed using the averaged pigment concentrations from each TP.
154 Analysis was performed essentially as described in Taylor et al. (2013). The initial pigment ratio
155 matrix, specific to North Pacific phytoplankton isolates, was taken from Table 5 in Lee et al.
156 (2011).

157 **2.4 Absorption spectra**

158 Absorption spectra of phytoplankton cellular pigments ($a_{\text{phy}}(\lambda)$) were determined following
159 the quantitative filter technique (QFT) as described in (Mitchell et al., 2002). At each TP,
160 duplicate 1.1 L samples were filtered onto pre-combusted 25 mm GF/F under low vacuum
161 pressure and light, taking care to achieve even sample distribution on the filter. Reference filters
162 were prepared by filtering 1.1 L of Milli-Q water. Filters were carefully placed into 25 mm tissue
163 capsules (Fisher), flash frozen in liquid nitrogen and stored at -80 °C until analysis within 1
164 month of the experiment. Sample filters were analyzed on a Cary BIO-100 dual-beam
165 spectrophotometer (Varian) against reference filters as described in Mitchell et al. (2002).
166 Optical density (OD) was measured from 370-800 nm (1 nm resolution) before and after
167 extraction of pigment with 90% methanol (Kishino et al., 1985) to determine OD of the whole
168 particulate sample and OD of detritus after pigment extraction, respectively. Each sample and
169 blank was analyzed in triplicate, to minimize error associated with instrument measurements.
170 The wavelength-specific phytoplankton pigment absorption spectrum ($a_{\text{phy}}(\lambda)$, m^{-1}) was
171 calculated as:

172
$$a_{phy}(\lambda) = 2.303 \times \left(OD_{sample}(\lambda) - OD_{detrius}(\lambda) \right) \times \frac{A}{V} \times \beta^{-1} \quad (2)$$

173 where 2.303 is the conversion of from base-10 to a natural logarithm, A is the particulate
174 retention area of the filter (m²), V is the volume filtered (m³), and β is the path-length
175 amplification coefficient (4.5; Röttgers and Gehrke, (2012)). To determine chl *a* specific
176 absorption spectra ($a^*_{phy}(\lambda)$, m⁻¹ mg chl *a*⁻¹), values were normalized to corresponding [chl *a*]
177 values. Absorption spectra were used for spectral correction of our rate measurements, as
178 described in detail below.

179 **2.5 FRRF-derived photophysiological parameters and ETR_{RCII}**

180 All FRRF measurements were conducted on a bench top FRRF instrument (Soliense Inc.), as
181 described in Schuback et al. (2015). *At each TP, background fluorescence blanks were prepared*
182 *by gently syringe filtering a small amount of sample through a pre-combusted GF/F.* We applied
183 a single turnover (ST) protocol *consisting of an excitation sequence* (100 flashlets with 1.0 μs
184 length and 2.5 μs interval, 46200 μmol quanta⁻² s⁻¹ peak power intensity, resulting in a
185 excitation sequence of 250 μs, providing ~5-10 quanta per RCII), *followed by a relaxation*
186 *sequence (50 flashlets with 1.0 μs length and 20 μs interval).* Excitation power was provided by
187 an array of eight LEDs at four wavelengths centered on 445 nm, 470 nm, 505 nm, and 530 nm
188 (equal intensity from each wavelength, *applied simultaneously*). We measured steady state light
189 curves (SSLC), where each sample was exposed to 10 actinic ‘background’ irradiances from 0 to
190 1000 μmol quanta m⁻² s⁻¹, provided at the same four wavelengths. All ChlF yields and
191 parameters described below were derived by an iterative non-linear fitting procedure, applying
192 the four parameter biophysical model of Kolber et al. (1998) to a mean of 20 consecutive ST
193 flashlet sequences using custom software (Z. Kolber). This software accounts for the formation
194 of fluorescence quenching, most likely due to formation of a P680 triplet, which reduces the
195 maximum fluorescence yield attainable during the ST flash by 3-6%. Throughout the SSLC, ST
196 flashlet sequences were measured continuously (1 s interval) and the length of each light step
197 was optimized to allow all derived parameters to reach steady state (ca 3 min). ChlF yields and
198 parameters corresponding to each light level were obtained from the mean of the last three
199 acquisitions at each light level. In this way, we derived the fluorescence yields F₀ and F_m (in

200 dark-regulated state) as well as F' and F_m' (in the light regulated state for each light level of the
 201 SSLC). F_o' was calculated as $F_o' = F_o / (F_v / F_m + F_o / F_m')$ (Oxborough and Baker, 1997).

202 The five fluorescence yields F_o , F_m , F' , F_m' and F_o' were used to calculate ChlF parameters,
 203 following Roháček (2002) as described in Schuback et al. (2015). Furthermore, the functional
 204 absorption cross section of PSII, σ_{PSII} ($\times 10^{-20}$ m² RCII⁻¹), was derived from the rate of closure of
 205 RCII in the dark-regulated and each light-regulated state (Kolber and Falkowski, 1993; Kolber et
 206 al., 1998). We calculated ETR_{RCII} as:

$$207 \quad ETR_{RCII} = E \times \sigma'_{PSII} \times \frac{F_q'}{F_v'} \times \Phi_{RC} \times 6.022 \times 10^{-3} \quad (3)$$

208 where E ($\mu\text{mol quanta m}^{-2} \text{s}^{-1}$) is the actinic irradiance at each light level, σ'_{PSII} ($\times 10^{-20}$ m² RCII⁻¹)
 209 is the functional absorption cross section of PSII at each light level, and F_q'/F_v' is the quantum
 210 efficiency of photochemical energy conversion in RCII at a given light intensity. The parameter
 211 F_q'/F_v' can also be interpreted as an estimate of the fraction of RCII in the open state, i.e. the
 212 primary stable electron acceptor in the oxidized state (Roháček, 2002). The parameter Φ_{RC} (mol
 213 e⁻ mol photon⁻¹) has the constant value of 1, given that for each photon absorbed and delivered to
 214 RCII, one electron is transferred from P₆₈₀ to Q_A (Kolber and Falkowski, 1993). The number
 215 6.022×10^{-3} converts $\mu\text{mol quanta}$ to quanta and 10^{-20} m² to m².

216 We additionally calculated ETR_{RCII} using the alternative approach

$$217 \quad ETR_{RCII} = E \times \sigma_{PSII} \times \frac{(F_q'/F_m')}{(F_v'/F_m)} \times \Phi_{RC} \times 6.022 \times 10^{-3} \quad (4)$$

218 Both calculations are equivalent, assuming that non-photochemical quenching processes
 219 affecting ChlF can be adequately accounted for in either the absorption term (Eq. 3) and the
 220 efficiency term (Eq. 4). The difference between ETR_{RCII} values calculated in both ways (n=71)
 221 was negligible, ranging from 1 % to 16 % with a mean coefficient of variance of 6 %.

222 The parameter τ (ms) is the time constant of re-oxidation of the primary stable electron
 223 acceptor Q_A and was estimated from the relaxation sequence of the ST protocol. We used values
 224 of τ , estimated for the dark-regulated state at each TP, to derive estimates of the rate of Q_A re-
 225 oxidation ($1/\tau$; ms⁻¹). Non-photochemical quenching (NPQ) at each light level was estimated as
 226 the so-called normalized Stern-Volmer quenching coefficient, $NPQ_{NSV} = (F_m'/F_v') - 1 = F_o'/F_v'$
 227 (McKew et al., 2013). This alternative approach to the more common estimate of NPQ ($(F_m -$

228 F_m'/F_m' ; Bilger and Björkman, 1990) represents the ratio of total non-photochemical energy
229 dissipation in the light-regulated state to the rate constant of photochemistry (McKew et al.,
230 2013).

231 **2.6 Carbon fixation**

232 Rates of carbon fixation were measured as small volume PvsE curves in a custom built
233 photosynthetron as described in Schuback et al. (2015). Briefly, 300 mL water samples were
234 spiked with 5.55 MBq NaH¹⁴CO₃ (final concentration 18.5 kBq mL⁻¹, 1.9425 GBq mL⁻¹ specific
235 activity) (Perkin-Elmer). All sample manipulations were conducted under low light. Samples
236 were spiked with tracer within 30 minutes of sampling, mixed gently but thoroughly, and then
237 aliquoted into 20 ml glass scintillation vials and placed into the photosynthetron. The total ¹⁴C
238 activity added was determined from three 1 mL aliquots of the spiked sample added to 1 mL of 1
239 M NaOH. Additionally, 3 time-zero samples were taken for each curve by filtering 20 mL
240 immediately after adding the spike. During the incubations, temperature was kept within 1 °C of
241 in situ temperature by circulating water from a water-bath through an aluminum cooling jacket.
242 Each PvsE curve consisted of 11 light levels spanning intensities from 3 to 600 μmol quanta m⁻²
243 s⁻¹. Incubations lasted for 3.5 hours and were ended by gentle filtration onto pre-combusted 25
244 mm GF/F filters. Given the length of the incubations and the likely slow growth rate of the iron-
245 limited phytoplankton assemblage sampled, our approach likely reflects a rate closer to net rather
246 than gross primary productivity (e.g. Halsey et al., 2011; Pei and Laws, 2013).

247 Filters were stored in scintillation vials at -20 °C until processing within 1 month of the
248 experiment. During laboratory processing, 500 μL of 3 M HCl was added to each filter and vials
249 were left to degas for >24 hours to eliminate any inorganic ¹⁴C remaining in the samples. Ten
250 mL of scintillation cocktail (Scintisafe plus, Fisher) were added to each vial, and vials were then
251 vortexed and left to stand in the dark for >12 hours before analysis on a liquid scintillation
252 counter (Beckman). Disintegrations per minute (DPM) were derived from scintillation counts
253 using a quench curve prepared from commercial ¹⁴C standards (Perkin-Elmer). DPM were
254 converted to units of carbon biomass following Knap et al. (Knap et al., 1996).

255 **2.7 Spectral correction and curve-fitting**

256 To account for differences in the spectral distribution of LEDs used in photosynthetron and
257 FRRF instrument, all rates were divided by a spectral correction factor (SCF).

$$258 \quad SCF = \frac{\sum_{400}^{700} a_{phy}^*(\lambda) E_{in\ situ}(\lambda) \sum_{400}^{700} E_{LED}(\lambda)}{\sum_{400}^{700} a_{phy}^*(\lambda) E_{LED}(\lambda) \sum_{400}^{700} E_{in\ situ}(\lambda)} \quad (5)$$

259 where $a_{phy}^*(\lambda)$ (m^{-1}) is the [chl *a*] specific phytoplankton pigment absorption spectrum
 260 determined for each TP as described above, E_{LED} is the spectral distribution of the LEDs used in
 261 photosynthetron or FRRF, and E_{insitu} is the spectral distribution of sunlight at 5 m depth. We
 262 estimated the in situ spectral distribution of PAR at 5 m depth following Stomp et al., 2007 as

$$263 \quad E(\lambda, z) = E_0(\lambda) \exp(-[K_w(\lambda) + K_{GT}(\lambda) + K_{PH}(\lambda)]z). \quad (6)$$

264 Here, $E_0(\lambda)$ is the spectral distribution of incident sunlight and $K_w(\lambda)$ (m^{-1}) is the absorption
 265 by pure water (Pope and Fry, 1997). $K_{GT}(\lambda)$ (m^{-1}) is the absorption by dissolved and particulate
 266 organic matter, estimated as $K_w(\lambda) = K_{GT}(440) \exp(-S(\lambda - 440))$, assuming that
 267 $K_{GT}(440) = 0.003 m^{-1}$, a typical value of clear open ocean water (Morel et al., 2007), and $S = 0.017$
 268 nm^{-1} (Kirk, 2010). Values for $K_{PH}(\lambda)$ (m^{-1}) were taken from the absorption spectra measured
 269 using the filter pad technique as described above.

270 After spectral correction, carbon fixation and ETR_{RCII} data were plotted against irradiance
 271 and fit to the exponential model of Webb et al. (1974) using a non-linear least squares regression
 272 procedure in MATLAB. For the carbon fixation data, an intercept parameter was added to force
 273 the regression through the origin and provide a good fit in the linear part of the $P_{vs}E$ curve
 274 (Arrigo et al., 2010; Suggett et al., 2001). For both rates of productivity, we derived the light
 275 saturated maximum rate P_{max} ($P_{max-ETR_{RCII}}$ and P_{max-C}), the light utilization efficiency α ($\alpha-$
 276 ETR_{RCII} and $\alpha-C$), and the light saturation point $E_k = P_{max}/\alpha$. When photoinhibition was observed
 277 at high irradiances, the data-points were excluded from the fitting procedure.

278 **2.8 Derivation of conversion factor**

279 The conversion factor linking ETR_{RCII} ($mol\ e^- mol\ RCII^{-1}\ s^{-1}$) and carbon fixation ($mol\ C\ mol$
 280 $chl\ a^{-1}\ s^{-1}$), was derived as described in Schuback et al. (2015);

$$281 \quad \frac{ETR_{RCII} (mol\ e^- mol\ RCII^{-1}\ s^{-1})}{C-fixation (mol\ C\ mol\ chl\ a^{-1}\ s^{-1})} = K_c \left(\frac{mol\ e^-}{mol\ C} \right) \times 1/n_{PSII} \left(\frac{mol\ chl\ a}{mol\ RCII} \right) \quad (6)$$

282 In this approach, the conversion factor between the two rates accounts for changes in chl *a*
 283 functionally associated with each RCII ($1/n_{PSII}$, $mol\ chl\ a\ mol\ RCII^{-1}$), as well as variability in

284 the number of charge separations in RCII per CO₂ assimilated (K_c , mol e⁻ mol C⁻¹). Reported
285 values for K_c range from 1.15 – 54.2 mol e⁻ mol C⁻¹ (Lawrenz et al., 2013) and 200 – 950 mol chl
286 a mol RCII⁻¹ for $1/n_{PSII}$ (Suggett et al., 2010). Consequently, values of K_c/n_{PSII} could be expected
287 to range from 230 - 51490 mol e⁻ mol C⁻¹ mol chl a mol RCII⁻¹.

288 Based on the measured light dependence of carbon fixation and ETR_{RCII} for each sample, we
289 were able to derive the light dependency of the conversion factor K_c/n_{PSII} at each TP.
290 Additionally, we used α and P_{max} values from the ETR_{RCII} and ¹⁴C PvsE curves to derive the
291 conversion factor under sub-saturating and saturating light conditions, respectively.

292 **2.9 Relative changes in $1/n_{PSII}$**

293 Combining two unknown variables (K_c and $1/n_{PSII}$) into one conversion factor, as described
294 above, limits our ability to physiologically interpret observed changes in the coupling of carbon
295 fixation and photosynthetic electron transport. An approach to estimate values of $1/n_{PSII}$ directly
296 from FRRF measurements has been developed by Oxborough et al. (2012). However, this
297 approach relies on the assumption that the ratio of the rate constants of photochemistry (k_p) and
298 fluorescence (k_f) stay within a narrow range. This assumption is invalidated under conditions of
299 iron limitation, where k_p decreases while k_f increases (e.g. Vassiliev et al., 1995), likely due to
300 the expression of light harvesting complexes that are energetically decoupled from RCII
301 (Behrenfeld and Milligan, 2013; Schrader et al., 2011). Consequently, the approach of
302 Oxborough et al. (2012) should be used with caution when comparing samples over a range of
303 iron limiting conditions.

304 In the current diurnal study, it is likely that the degree of iron limitation experienced by the
305 phytoplankton assemblage stayed relatively constant during our sampling period, such that k_p/k_f
306 values would have remained within a narrow range. Using this rationale, we applied a simplified
307 version of the Oxborough et al. (2012) approach to our data, allowing us to estimate relative
308 diurnal changes in $1/n_{PSII}$, and, by deduction K_c . In the original approach by Oxborough et al.
309 (2012), changes in F_o/σ_{PSII} , measured in the dark-regulated state, are multiplied by an
310 instrument specific calibration factor (K_R) to derive absolute values of [RCII]. Lacking this
311 instrument specific calibration factor K_R , we were not able to derive absolute values for [RCII]
312 (and in turn $1/n_{PSII}$). However, since K_R is presumed to be constant, we used F_o/σ_{PSII} measured in
313 the dark regulated state at each TP to derive an estimate of relative [RCII] values. These relative

314 [RCII] values were then normalized to [chl *a*] to estimate diurnal changes in $1/n_{PSII}$, which were,
315 in turn, used to estimate relative diurnal changes in K_c . from measurements of K_c/n_{PSII} .

316 **3 Results**

317 **3.1 Physical and chemical characteristics of the water-column during the** 318 **experiment**

319 During the sampling period, the upper water-column at OSP was stratified, with a well-defined
320 mixed layer of 33 ± 2 m. As expected for iron-limited waters, excess macronutrients were
321 present in the mixed layer and concentrations did not vary over the course of our sampling (2
322 casts, 3:30 and 12:30 local time; $N = 9.1 \pm 0.00 \mu\text{mol L}^{-1}$, $P = 0.98 \pm 0.01 \mu\text{mol L}^{-1}$, and $Si =$
323 $14.5 \pm 0.51 \mu\text{mol L}^{-1}$). Chlorophyll *a* concentrations were homogenously distributed throughout
324 the mixed layer ($0.26 \pm 0.03 \text{ mg m}^{-3}$; 8 depths sampled on 1 cast at 12:30 local time), while
325 temperature was nearly invariant ($10.4 \pm 0.07 \text{ }^\circ\text{C}$) during our sampling period. Total daily
326 incident PAR dose over the 24 h period (E_0^+) was **31.94 mol quanta m^{-2}** , with a noon maximum
327 of $1,162 \mu\text{mol quanta}^{-2} \text{ s}^{-1}$. The water column light extinction coefficient, k_d , was 0.07 m^{-1} ,
328 which is a value typical for the open ocean (Kirk, 2010). The photic zone (**defined as the 0.1%**
329 **light level**) extended below the mixed layer depth at all TPs, apart from the nighttime TP (TPs 1,
330 7 and 8).

331 **3.2 Phytoplankton community composition**

332 CHEMTAX analysis of the pigment data suggested that the phytoplankton assemblage at the
333 sampling location was highly diverse, consisting of approximately 3% diatoms, 2%
334 dinoflagellates, 15% prymnesiophytes, 12% chlorophytes, 16% prasinophytes, 14%
335 cryptophytes, 15% pelagophytes and 23% cyanobacteria.

336 **3.3 Diurnal changes in rates of carbon fixation and ETR_{RCII}**

337 Over the course of the diurnal cycle, we observed significant changes in the P_{vsE} curves for
338 carbon fixation and ETR_{RCII} (Fig. 1). However, the two rates, and their light dependency, did not
339 change in parallel (Fig. 1). As a consequence, we observed significant changes in magnitude and
340 light dependency of the derived conversion factor K_c/n_{PSII} . At all TP, K_c/n_{PSII} increased with

341 increasing light (Fig. 1). The maximum, light-saturated value of K_c/n_{PSII} as well as the slope of
342 the light dependent increase was highest in the afternoon, with maximum K_c/n_{PSII} values (>9000
343 $\text{mol e}^- \text{mol C}^{-1} \text{mol chl } a \text{ mol RCII}^{-1}$) observed (Fig. 1).

344 From the PvsE curves shown in Fig. 1 we derived the photosynthetic parameters P_{\max} and α for
345 both ETR_{RCII} and carbon fixation (Fig. 2c-f). Over the diurnal cycle, the $P_{\max}\text{-ETR}_{\text{RCII}}$ changed
346 by a factor of 3.2 and closely followed the incident irradiance (Fig. 2c), with peak values
347 observed around solar noon. In contrast, $P_{\max}\text{-C}$ was highest in the early morning and then
348 steadily declined over the course of the day, changing by a factor of 2.5 over the diurnal cycle
349 (Fig. 2e). The conversion factor K_c/n_{PSII} , derived for light saturated photosynthesis ($P_{\max}\text{-}$
350 $\text{ETR}_{\text{RCII}}/P_{\max}\text{-C}$), exhibited high values and a pronounced diurnal cycle, varying by a factor of 2.9
351 (Fig. 2g). Minimum values of K_c/n_{PSII} were observed early in the morning, while maximum
352 values were observed during the afternoon.

353 The light use efficiency per incident quanta under sub-saturating light conditions, α , showed
354 similar patterns to P_{\max} for both ETR_{RCII} and carbon fixation (Fig. 2). Values for $\alpha\text{-ETR}_{\text{RCII}}$
355 peaked during the late morning and then declined during the afternoon and into the evening (Fig.
356 2d). In contrast, $\alpha\text{-C}$ was highest before sunrise and steadily decreased throughout the day (Fig.
357 2f). Over the course of the diurnal cycle, $\alpha\text{-ETR}_{\text{RCII}}$ changed by a factor of 1.9 while $\alpha\text{-C}$
358 changed by a factor of 3.1. As with P_{\max} , the conversion factor K_c/n_{PSII} derived for α , varied
359 strongly (2.4 fold) over the diurnal cycle and showed maximum values during the afternoon, in
360 conjunction with the highest incident PAR levels (Fig. 2h). At all TP, the conversion factor
361 K_c/n_{PSII} was higher during light saturated photosynthesis (P_{\max}) than under conditions of light
362 limitation (α) (Fig. 2g and 2h, note different scale of y-axis).

363 The light saturation point E_k was higher for ETR_{RCII} than for carbon fixation at all TPs
364 (Fig. 3), implying that carbon fixation rates saturated at lower light intensity than ETR_{RCII} . For
365 both, carbon fixation and ETR_{RCII} , P_{\max} and α changed roughly in parallel (Fig. 2 c, d and 2 e, f).
366 Consequently, diurnal changes in E_k , derived as P_{\max}/α , were relatively small (Fig. 2i).
367 Furthermore, the relatively low values of E_k ($\sim 100 - 150 \mu\text{mol quantam}^{-2} \text{s}^{-1}$) indicate that both,
368 ETR_{RCII} and carbon fixation, were saturated at in situ irradiance levels for most of the day (Fig.
369 2i).

370 Using the PvsE curves measured for both ETR_{RCII} and carbon fixation (Fig. 1), we derived rates
371 corresponding to the in 5 m irradiance levels at each TP (Figs. 3b and 3c). Over the diurnal

372 cycle, these derived in situ rates of ETR_{RCII} changed by a factor of 5.1 (Fig. 3b), closely
373 following changes in ambient irradiance levels (Fig. 3a), with peak values around noon. By
374 comparison, carbon fixation derived for in situ light levels at 5 m depth changed by a factor of
375 1.7 over the period of our sampling (Fig. 3c). The maximum rate of realized carbon fixation at 5
376 m depth (0.0433 ± 0.0112 mol C mol chl $a^{-1} s^{-1}$) was reached in the morning, well before the
377 daily irradiance maximum (Figs. 3a and 3c). The derived in situ conversion factor K_c/n_{PSII} varied
378 by a factor of 3.4. Lowest derived values of in situ K_c/n_{PSII} were observed early in the morning
379 after which values increased until reaching a maximum in the afternoon (Fig. 3d).

380 **3.4 Relative changes in $1/n_{PSII}$**

381 Relative values of $1/n_{PSII}$, shown in Fig. 4a, were highest in the early morning, and then
382 declined by 37% through the afternoon, with lowest values observed at midnight (Fig. 4a). The
383 magnitude of diurnal change in $1/n_{PSII}$ was significantly less than the diurnal changes observed
384 in K_c/n_{PSII} , which were 245% at in situ irradiances (Fig. 4b), 185% at light saturation (P_{max} ; Fig.
385 4c) and 138% at light limitation (α , Fig. 4d). We examined K_c -specific variability by
386 normalizing K_c/n_{PSII} estimates to the relative changes in $1/n_{PSII}$. As shown in Fig. 4, the derived
387 relative changes in K_c showed a diel pattern very similar to that observed for K_c/n_{PSII} at in situ
388 irradiances (Fig. 4b), at light saturation (P_{max} , Fig 4c), and under light limitation (α , Fig. 4d).
389 This result indicates that changes in K_c were the primary drivers of observed variability in
390 K_c/n_{PSII} .

391 **3.5 Photo-regulatory changes**

392 In addition to the apparent diurnal changes in carbon fixation and ETR_{RCII} , we observed strong
393 diurnal oscillations in a number of photophysiological parameters, as well as changes in pigment
394 composition of the phytoplankton assemblage. *While higher resolution pigment data would have
395 been desirable*, the changes in pigment ratios shown in Fig. 5 indicate that the phytoplankton
396 assemblage sampled from 5 m depth experienced supersaturating light conditions for a
397 substantial part of the day.

398 The ratio of photo-protective carotenoids (PPC) to total pigment (TPig), changed by a factor of
399 1.4 over the diurnal cycle, *with lowest values observed at the pre-dawn TP (3:00) and highest in
400 the afternoon (15:00) (Fig. 5a)*. Similarly, the proportion of xanthophyll cycling (XC) pigments
401 *to total chl a increased from pre-dawn (3:00) to mid-afternoon (15:00)*. This increase was

402 observed in XC pigments specific to chromophytes (42% increase in $(Dd+Dt)/chl\ a$, Fig. 5b) as
403 well as chlorophyte and prasinophyte-specific XC pigments (17% increase in $(Zea+Viol)/chl\ a$,
404 Fig 5c). Changes in relative abundance of XC pigments indicate that a higher proportion of the
405 pigment pool is dedicated to photoprotection.

406 In addition to changes in XC pigments, we also observed a 2.4-fold increase in the DES ratio
407 $(Dt/(Dd+Dt))$ of chromophyte algae between 3:00 and 15:00 (Fig. 5b), and a 1.8-fold increase in
408 the DES ratio of chlorophytes and prasinophytes $(Zea/(Zea+Viol))$, Fig. 5c. The changes in the
409 DES ratio are an indicator of the activation of the photoprotective XC process (Brunet et al.,
410 2011). Our results should be considered as conservative estimates of the DES ratios, given the
411 potential for reversal of the high light induced de-epoxidation during sample processing (samples
412 were exposed to low light for approx. 30 – 60 min during sample collection and filtration).
413 Notwithstanding the relatively low temporal resolution of our pigment samples, the observed
414 changes in pigment ratios indicate that the phytoplankton assemblage sampled from 5 m depth
415 experienced super-saturating light conditions for a substantial part of the day.

416 Further evidence for super-saturating light conditions in the mixed layer comes from
417 observations of diurnal changes in PSII-specific photophysiological parameters derived from
418 FRRF measurements (Fig. 6). Values of F_v/F_m , measured in the dark-regulated state, varied from
419 0.12 to 0.32 and showed an inverse relationship to irradiance (Fig. 6a), likely indicating down-
420 regulation or damage of PSII during high irradiance conditions. The parameter $1/\tau$ (ms^{-1}) is an
421 estimate of the rate of electron transfer from the first stable electron acceptor Q_A to the second
422 stable electron acceptor Q_B . Values of $1/\tau$ varied in parallel with available irradiance over the
423 diurnal cycle, changing approximately 3-fold, and indicating faster electron transport
424 downstream of charge separation in RCII during daylight hours (Fig. 6b). Estimates of the
425 expression of non-photochemical quenching, NPQ_{NSV} , at in situ (5 m depth) irradiance levels
426 changed 7.6-fold over the diurnal cycle, with maximum values near the peak of solar irradiance
427 (Fig. 6c). Spectrally corrected values of the functional absorption cross section of PSII, σ'_{PSII} ,
428 also derived for in situ irradiance levels, correlated inversely with irradiance (Fig. 6d). This
429 decrease further confirms the induction of photo-protective mechanisms within the pigment
430 antenna, preventing excess energy from reaching RCII. Photochemical quenching, estimated as
431 F_q'/F_v' , indicates the fraction of RCII in the 'open state', with the primary stable electron
432 acceptor Q_A in the oxidized state (Roháček, 2002). Values of F_q'/F_v' , derived for a reference

433 irradiance value of $500 \mu\text{mol quanta m}^{-2} \text{ s}^{-1}$ at all TP (F_q'/F_v' (500)), show significant change
434 over the diurnal cycle, with mid-day values twice as high as those observed during the night (Fig.
435 6e).

436 **4 Discussion**

437 The experimental approach and results presented in this study confirm the hypothesized diurnal
438 variation in the coupling of ETR_{RCII} and carbon fixation under iron-limited conditions.

439 Building on the work of others (Behrenfeld et al., 2004, 2008; Halsey and Jones, 2015) we
440 interpret our results in the context of environmentally driven shifts in cellular energy allocation,
441 which decouple photosynthesis from net growth on diurnal timescales. We speculate that the
442 observed patterns are caused by photophysiological plasticity on a molecular level, which
443 enables phytoplankton to maximize growth while minimizing photodamage under iron-limited
444 conditions.

445 In the following, we first discuss diurnal variation at the level of carbon fixation and put our
446 observations in context with the rich information available from the literature. We then consider
447 the diurnal changes in ETR_{RCII} and the derived conversion factor K_c/n_{PSII} , and discuss the
448 relevance of our results to the development of FRRF-based phytoplankton primary productivity
449 measurements.

450 **4.1 Diurnal changes in carbon fixation**

451 Diurnal variations in the capacity ($P_{\text{max-C}}$), efficiency ($\alpha\text{-C}$) and realized rates of carbon
452 fixation are characteristic of phytoplankton assemblages in the natural environment, and in
453 laboratory cultures (Bruyant et al., 2005; Doblin et al., 2011; Doty and Oguri, 1957; Erga and
454 Skjoldal, 1990; Harding et al., 1981, 1982, 1987; John et al., 2012; MacCaull and Platt, 1977;
455 Prézelin, 1992; Stross et al., 1973; Zhao and Quigg, 2015). The general consensus is that carbon
456 fixation is not passively regulated by the availability of light, but by complex metabolic
457 feedbacks and endogenous circadian rhythms.

458 For example, it has been shown that expression of genes involved in carbon fixation peaks
459 before dawn (Ashworth et al., 2013; Granum et al., 2009), 'priming' cells to achieve maximum

460 rates early in the day. High carbon fixation capacities ($P_{\max-C}$) before sunrise, as observed in our
461 data (Fig. 2e), further confirm endogenous circadian control of this pathway.

462 In our data, $P_{\max-C}$ and $\alpha-C$ peaked early in the morning and co-varied over the diurnal cycle
463 (Fig. 2e and 2f). As a result, E_k (which is derived from the ratio of these parameters) remained
464 relatively constant (Fig. 2i). This ‘ E_k -independent’ variability in the photosynthetic parameters
465 $P_{\max-C}$ and $\alpha-C$ has long been considered somewhat enigmatic, but is now accepted to be driven
466 by shifts in cellular energy allocation (Behrenfeld et al., 2004, 2008; Bruyant et al., 2005; Halsey
467 and Jones, 2015). In phytoplankton, the fraction of photosynthetically-derived reductant
468 (NADPH) and energy equivalent (ATP) allocated to carbon fixation and net growth as well as
469 the ratio of NADPH:ATP produced are finely tuned to match metabolic demand. Metabolic
470 demand, in turn, is a function of evolved endogenous rhythms and external environmental
471 forcing. As discussed below, the decline in $P_{\max-C}$ (Fig. 2e), $\alpha-C$ (Fig. 2f), and realized rates of
472 carbon fixation (Fig. 3c) after a peak in the early morning, are likely due to such shifts in energy
473 allocation, and to the damaging effects of excess light, which accumulate throughout the light-
474 period.

475 **4.2 Diurnal changes in ETR_{RCII} and the conversion factor K_c/n_{PSII}**

476 In contrast to the diurnal cycles of $P_{\max-C}$ and $\alpha-C$, changes in $P_{\max-ETR_{RCII}}$ and $\alpha-ETR_{RCII}$
477 followed availability of light more closely, peaking around noon (Fig. 2 c,d). Similarly, realized
478 ETR_{RCII} , derived for in situ irradiances at each TP, correlated more closely to light availability
479 than realized rates of carbon fixation (Fig. 3b). While it has been demonstrated that virtually all
480 stages of photosynthesis exhibit circadian control (Suzuki and Johnson, 2001), our results
481 suggests that ETR_{RCII} responds more directly to changes in light availability than the subsequent
482 conversion of light energy into cellular organic carbon. It is important to note that the
483 accumulation of photo-damage and inhibition over the course of the light-period is likely to
484 impart some level of hysteresis to diurnal changes in ETR_{RCII} . Relative to carbon fixation,
485 however, our results show that ETR_{RCII} is much more closely tied to instantaneous changes in
486 light availability. The resulting decoupling of carbon fixation and photosynthetic electron
487 transport is reflected in the diurnal variability in K_c/n_{PSII} (Figs. 2g, 2h, 3d). Based on our
488 estimates of relative changes in $1/n_{PSII}$ over the diel cycle (Fig. 4), we conclude that the majority
489 of diurnal variability in K_c/n_{PSII} results from changes in K_c .

490 In our dataset, in situ values for K_c/n_{PSII} ranged from 2700 to 9200 mol e⁻ mol C⁻¹ mol chl *a* mol
491 RCII⁻¹. Assuming a constant $1/n_{PSII}$ of 500 mol chl *a* mol RCII⁻¹ (Kolber and Falkowski, 1993),
492 the derived K_c ranges from 5-18 mol e⁻ mol C, which is within the range of previously reported
493 values (Lawrenz et al., 2013) and above the theoretical minimum of 4 mol e⁻ mol C.

494 The large diurnal variability in ETR_{RCII} and carbon fixation and the highly variable K_c/n_{PSII} ,
495 reflect the integrated growth environment experienced by the sampled phytoplankton
496 assemblage. The lowest values of K_c/n_{PSII} were observed early in the morning (Fig. 3d),
497 indicating that much of the energy harvested from sunlight and converted into chemical energy
498 was used directly for carbon fixation. Thereafter, the conversion factor K_c/n_{PSII} increased rapidly,
499 reaching a maximum in the afternoon (Fig. 3d).

500 Diurnal variation in K_c/n_{PSII} can result from a number of interconnected cell physiological
501 mechanisms aimed at re-balancing of energy and/or reductant. Firstly, it is possible that diurnal
502 oscillations in cell metabolism result in changes inorganic carbon respiration and/or excretion. In
503 our 3.5 hours ¹⁴C-uptake experiments, transient organic carbon pools destined for respiration or
504 excretion could have been captured to different extents, affecting the derived conversion factor
505 K_c/n_{PSII} . Changes in cellular energy allocation, controlled in part by endogenous circadian
506 rhythms, could also have affected the conversion factor K_c/n_{PSII} , by re-routing NADPH and ATP
507 generated by the photosynthetic light reaction to processes other than carbon fixation, thus
508 increasing K_c/n_{PSII} . Processes decoupling ETR_{RCII} from carbon fixation include nutrient
509 assimilation (Laws, 1991), carbon concentrating mechanisms (Giordano et al., 2005),
510 photorespiration (Foyer et al., 2009), and malate formation (Halsey and Jones, 2015). Pseudo-
511 cyclic electron transport through the Mehler-ascorbate peroxidase pathway also has the ability to
512 increase the conversion factor K_c/n_{PSII} by allowing ETR_{RCII} to increase without affecting carbon
513 fixation (Miyake and Asada, 2003; Niyogi, 2000). Moreover, processes acting before PSI can
514 decouple ETR_{RCII} and carbon fixation by ‘siphoning’ electrons out of the ETC to alleviate over-
515 reduction under supersaturating light condition. Pseudo-cyclic electron transport through
516 midstream terminal oxidases (Bailey et al., 2008; Mackey et al., 2008), cyclic electron transport
517 around PSII (Feikema et al., 2006; Prasil et al., 1996), and charge recombination in RCII (Vass,
518 2011) could all be important under high mid-day irradiances, increasing ETR_{RCII} without
519 affecting CO₂-assimilation, and thus leading to a higher conversion factor K_c/n_{PSII} .

520 Iron limitation, as experienced by the phytoplankton assemblage we sampled, directly affects
521 the functioning of the ETC, which is rich in iron containing redox-chain components (Raven et
522 al., 1999; Yruela, 2013). It is thus likely that the need for safe dissipation of excess excitation
523 pressure after charge separation in RCII is enhanced under iron limitation (Behrenfeld and
524 Milligan, 2013; Schuback et al., 2015), leading to a greater decoupling of ETR_{RCII} and carbon
525 fixation (Schuback et al., 2015). Pseudo-cyclic electron flow could alleviate over-reduction of
526 the ETC under iron limiting conditions, while also contributing to ATP production (Behrenfeld
527 and Milligan, 2013). The resulting increase in the cellular ATP:NADPH ratio would match the
528 shift in energy demand from growth (higher NADPH requirement) to maintenance (higher ATP
529 requirement), which takes place under nutrient limited growth conditions.

530 While the exact nature and extent of operation of these various pathways and their actual
531 influence on the coupling of ETR_{RCII} and carbon fixation remains to be verified, we suggest that
532 the observed changes in the conversion factor K_c/n_{PSII} over the diurnal cycle reflect the
533 interactions of external phasing of photosynthetic metabolism by the availability of light and
534 internal metabolic rhythms in cell metabolism, which optimize energy allocation and growth
535 under iron-limited conditions.

536 **4.3 Diurnal changes in photophysiology at the level of PSII**

537 In our data, several lines of evidence demonstrate that the phytoplankton assemblage we
538 sampled from 5 m depth experienced supersaturating irradiance during part of the day. A suite of
539 mechanisms was activated to dissipate the excess excitation energy in the pigment antenna,
540 before it could reach RCII. This was indicated by changes in pigment ratios (Fig. 5) and FRRF-
541 derived photophysiological parameters (Fig. 6). The light harvesting antennae of phytoplankton
542 are comprised of both photosynthetic and photoprotective pigments, the relative abundance of
543 which can change in response to irradiance. The ratio $[PPC]/[TPig]$, provides information on the
544 degree of high light acclimation of a mixed phytoplankton assemblage (Brunet et al., 2011). In
545 our data, $[PPC]/[TPig]$ increased during the day (Fig. 5a), indicating that the phytoplankton
546 assemblage experienced and responded to supersaturating irradiance levels. Furthermore,
547 significant changes in the DES ratio of chromophytes ($Dt/(Dt+Dd)$, Fig. 5b), as well as
548 chlorophytes and prasinophytes ($Zea/(Zea+Viol)$, Fig. 5c) illustrate rapid activation of

549 photoprotective energy dissipation in the pigment antenna in response to diurnal changes in
550 irradiance (Brunet et al., 2011).

551 Figure 6 shows pronounced diurnal variability in a number of FRRF derived parameters. Both
552 F_v/F_m (Fig. 6a) and $1/\tau$ (Fig. 6d) were derived for the dark-regulated state at each TP. To reach
553 this dark-regulated state, samples were kept under very low light for a minimum of 30 minutes
554 prior to the measurement. In theory, such low-light incubation allows for oxidation of the ETC
555 and relaxation of all NPQ processes, enabling the measurement of maximum ChlF yields. In
556 practice, however, a fully dark-regulated state cannot be achieved in natural phytoplankton
557 assemblages, where optimal dark-acclimation times can be on the order of hours long (From et
558 al., 2014), and would depend on recent light history and taxonomic composition. Consequently,
559 the interpretation of ChlF yields and parameters in field phytoplankton assemblages should be
560 treated with caution. Notwithstanding these caveats, the FRRF-derived ChlF yields and
561 parameters shown in Fig. 6 show clearly that, at the level of PSII, the sampled phytoplankton
562 assemblage experienced and reacted to excess irradiance.

563 While it is known that nutritional state and taxonomy both strongly influence values of F_v/F_m
564 (Suggett et al., 2009), it is very unlikely that changes in either are responsible for pronounced
565 diurnal cycle of F_v/F_m observed in our data (Fig. 6a). We therefore attribute the mid-day decrease
566 in F_v/F_m to persistent photo-protective changes and photoinhibition in PSII (Öquist et al., 1992).

567 Processes including the light-induced changes in pigment composition shown in Fig. 5, act to
568 dissipate excess excitation pressure in the pigment antenna, before reaching RCII. These
569 processes also quench ChlF yields, as measured by FRRF. Consequently, so-called non-
570 photochemical quenching (NPQ), as estimated from FRRF measurements, has been widely used
571 as an estimate for photoprotective energy dissipation (Demmig-Adams et al., 2014; Derks et al.,
572 2015). NPQ encompasses a wide variety of mechanisms, all acting to dissipate absorbed light
573 energy as heat before it reaches RCII (e.g. Derks et al., 2015). Following the approach of
574 McKew et al. (2013) we estimated NPQ from FRRF measurements as so-called normalized
575 Stern-Volmer quenching (NPQ_{NSV}). The 7.6-fold change in NPQ_{NSV} , estimated for in situ light
576 availability at 5 m depth (Fig. 6b), confirms that the phytoplankton assemblage sampled
577 experienced, and rapidly reacted to, super-saturating light conditions. The inverse light
578 dependence of the functional absorption cross-section of PSII, σ'_{PSII} , derived for in situ

579 irradiances at each TP (Fig. 6c), provides a further illustration of rapid changes taking place in
580 the pigment antenna to prevent excess excitation energy from reaching RCII.

581 In addition to the protective mechanisms acting in the pigment antenna to prevent charge
582 separation in RCII, photo-protective mechanisms also act after charge separation in RCII
583 (section 4.2). These mechanisms alleviate over-reduction by allowing rapid re-oxidation of the
584 primary stable electron acceptor Q_A . Our data show evidence of the up-regulation of such
585 alternative electron sinks during mid-day. Figure 6d shows a light-dependent increase in $1/\tau$,
586 which provides an estimate of the rate of re-oxidation of the first stable electron acceptor Q_A .
587 Increased $1/\tau$ thus suggests faster electron flow downstream from Q_A , which is consistent with
588 the up-regulation of alternative electron sinks. Further support for this idea comes from diel
589 changes in the estimated fraction of Q_A in the oxidized state (F_q'/F_v'), derived for a reference
590 irradiance of $500 \mu\text{mol quanta m}^{-2} \text{ s}^{-1}$ (Fig. 6e). The mid-day increase in the oxidized fraction of
591 Q_A at a constant saturating irradiance of $500 \mu\text{mol quanta m}^{-2} \text{ s}^{-1}$ strongly suggests the up-
592 regulation of alternative electron sinks, which most likely serve a photoprotective function
593 (Mackey et al., 2008). Up-regulation of these photo-protective mechanisms, influences the
594 coupling between electron transport and carbon fixation, and thus directly affects the conversion
595 factor K_c/n_{PSII} (section 4.2).

596 **4.4 Linking K_c/n_{PSII} and NPQ_{NSV}**

597 Excess excitation energy leads to the induction of processes preventing energy transfer to RCII,
598 and to processes acting to prevent over-reduction of the ETC after charge separation. NPQ_{NSV}
599 provides an estimate of thermal energy dissipation upstream of RCII, which acts to prevent
600 excess electron transport and over-reduction of the ETC. Down-stream changes in electron flow
601 after charge separation at RCII are reflected in changes in K_c/n_{PSII} , through the induction of
602 various mechanism, as discussed in the previous section. Following the approach and
603 interpretation suggested by Schuback et al. (2015), we examined the correlation between the
604 derived conversion factor K_c/n_{PSII} and estimates of NPQ_{NSV} . For this analysis, we used estimates
605 of NPQ_{NSV} for each light level and TP of the FRRF light curves and derived values of K_c/n_{PSII} by
606 extrapolation along the carbon fixation and ETR_{RCII} based P_{vsE} curves. As shown in Fig. 7, we
607 found a strong correlation between these two variables ($R^2= 0.81$, $p\text{-value}<0.0001$, $n=64$).

608 As described in detail in Schuback et al. (2015), the observed empirical correlation between
609 K_c/n_{PSII} and NPQ_{NSV} can be rationalized in terms of photophysiological mechanisms, acting to
610 dissipate excess excitation energy both upstream and downstream of charge separation in RCII.
611 The dissipation of excess excitation energy as thermal energy before reaching RCII, estimated as
612 NPQ_{NSV} , prevents excess electron transport and over-reduction of the ETC. After the initial
613 charge separation in RCII, excess electron transport and over-reduction of the ETC can be
614 alleviated by a number of alternative electron pathways; the up-regulation of which will increase
615 K_c/n_{PSII} (e.g. Bailey et al., 2008; Cardol et al., 2011; Laureau et al., 2013; Mackey et al., 2008;
616 McDonald et al., 2011; Niyogi, 2000; Streb et al., 2005; Vass, 2011; Zehr and Kudela, 2009).
617 Thus, both NPQ_{NSV} and K_c/n_{PSII} respond strongly to excess excitation pressure, providing a
618 possible mechanistic interpretation for their correlation. In fact, a positive feedback loop exists
619 between energy dissipation in the antenna and photosynthetic control in the ETC, because
620 alternative electron pathways enhance the trans-membrane ΔpH , which triggers several
621 components of NPQ (Nawrocki et al., 2015). The correlation between NPQ_{NSV} and K_c/n_{PSII} is
622 likely to be especially strong under iron limiting conditions, due to the enhancement of energy
623 dissipation mechanisms when the functioning of the ETC is comprised by the availability of iron.
624 While a correlation between NPQ_{NSV} and K_c/n_{PSII} has important implications for the derivation
625 of carbon-based primary productivity rates from FRRF measurements, the correlation can be
626 confounded by ambiguity and inherent biases in the derivation of all involved parameters. For
627 example, while the correlations between NPQ_{NSV} and K_c/n_{PSII} in the present, as well as our
628 previously published dataset (Schuback et al., 2015), are strong, their regression slopes differ.
629 The observed discrepancy could be explained in several ways. Firstly, data in our previous study
630 was not corrected for spectral differences between the FRRF instrument, the ^{14}C -uptake
631 experiments and in situ light. As a consequence, absolute values of the derived conversion factor
632 were likely over-estimated. Furthermore, data presented in Schuback et al. (2015) included
633 phytoplankton assemblages sampled over a range of iron-limited and iron-replete conditions.
634 The resulting variability in phytoplankton growth rates influence the balance between net and
635 gross carbon fixation captured in 3 hour ^{14}C -uptake experiments (Halsey et al., 2011; Milligan et
636 al., 2015; Pei and Laws, 2013), and affect the derived conversion factor K_c/n_{PSII} .
637 More generally, significant uncertainty remains in the estimation of ETR_{RCII} from ChlF yields,
638 particularly if the theoretical biophysical models are applied to mixed phytoplankton

639 assemblages containing species with contrasting photosynthetic architectures and photo-
640 physiological characteristics. Inherent biases and potential systematic errors in the derivation of
641 ETR_{RCII} will inevitably affect the derived conversion factor K_c/n_{PSII} . Similarly, it remains unclear
642 if the quenching of ChlF yields, used to derive NPQ, correlate linearly with increases in thermal
643 energy dissipation in the pigment antenna (Derks et al., 2015). Ultimately, larger datasets,
644 spanning multiple oceanic regions and phytoplankton assemblages of contrasting taxonomic
645 composition and physiological state are needed to further investigate the correlation between
646 NPQ_{NSV} and K_c/n_{PSII} .

647 **5 Conclusion**

648 The lure of FRRF instruments lies in their potential for autonomous, instantaneous data
649 acquisition at high temporal and spatial resolution. However, uncertainty in the conversion
650 factor needed to convert rates of ETR_{RCII} into ecologically relevant rates of carbon fixation
651 remains a significant challenge. Through a suite of photo-physiological data and ancillary
652 measurements, our results provide some insight into the potential mechanistic causes leading to
653 an uncoupling of ETR_{RCII} and carbon fixation over diurnal cycles in iron-limited phytoplankton
654 assemblages. Beyond providing improved methods to estimate phytoplankton carbon fixation
655 rates, information on magnitude and variability of the conversion factor linking ETR_{RCII} and
656 carbon fixation allows a better mechanistic understanding of how phytoplankton harvest and
657 allocate light energy in response to environmental conditions. Our mechanistic understanding of
658 these processes is crucial for the modeling and prediction of patterns in marine primary
659 productivity in the face of climate-dependent changes in oceanic ecosystems.

660 More generally, it is important to consider that the dynamics of marine productivity over
661 long time-scales are ultimately controlled by interactions among biological and physical
662 processes that have strong diurnal components. Several recent studies suggest a previously
663 under-appreciated importance of closely coupled diurnal oscillations as the underlying
664 mechanisms of ecosystem stability in open ocean food webs (Ottesen et al., 2014; Ribalet et al.,
665 2015). Our results show strong diurnal variability in photophysiology and cell metabolism of
666 mixed phytoplankton assemblages. These physiological processes likely influence the phasing

667 and periodicity of higher trophic level processes, and may ultimately contribute to conveying
668 stability to the system.

669

670 **Acknowledgements**

671 The authors thank Marie Robert and the scientific and coast guard crews on board *CCGS*
672 *John P. Tully* during Line-P 2014-18. We would further like to thank Z. Kolber for assistance
673 with the FRRF instrument and C. Hoppe and D. Semeniuk for their critical reading of earlier
674 versions of the manuscript. We furthermore thank three anonymous reviewers for their insightful
675 comments and suggestions.

1 **References**

- 2 Arrigo, K. R., Mills, M. M., Kropuenske, L. R., Dijken, G. L. van, Alderkamp, A.-C. and
3 Robinson, D. H.: Photophysiology in two major southern ocean phytoplankton taxa:
4 photosynthesis and growth of *Phaeocystis antarctica* and *Fragilariopsis cylindrus* under
5 different irradiance levels, *Integr. Comp. Biol.*, 50, 950–966, doi:10.1093/icb/icq021, 2010.
- 6 Ashworth, J., Coesel, S., Lee, A., Armbrust, E. V., Orellana, M. V. and Baliga, N. S.: Genome-
7 wide diel growth state transitions in the diatom *Thalassiosira pseudonana*, *Proc. Natl. Acad.*
8 *Sci.*, 110, 7518–7523, doi:10.1073/pnas.1300962110, 2013.
- 9 Babin, M., Morel, A., Claustre, H., Bricaud, A., Kolber, Z. and Falkowski, P. G.: Nitrogen- and
10 irradiance-dependent variations of the maximum quantum yield of carbon fixation in eutrophic,
11 mesotrophic and oligotrophic marine systems, *Deep Sea Res. Part Oceanogr. Res. Pap.*, 43,
12 1241–1272, doi:10.1016/0967-0637(96)00058-1, 1996.
- 13 Bailey, S., Melis, A., Mackey, K. R. M., Cardol, P., Finazzi, G., van Dijken, G., Berg, G. M.,
14 Arrigo, K., Shrager, J. and Grossman, A.: Alternative photosynthetic electron flow to oxygen in
15 marine *Synechococcus*, *Biochim. Biophys. Acta BBA - Bioenerg.*, 1777, 269–276,
16 doi:10.1016/j.bbabi.2008.01.002, 2008.
- 17 Barwell-Clarke, F.W.: Institute of Ocean Sciences Nutrient Methods and Analysis, *Can. Tech.*
18 *Rep. Hydrogr. Ocean Sci.* , 182, 43 pp., 1996.
- 19 Behrenfeld, M. J. and Milligan, A. J.: Photophysiological expressions of iron stress in
20 phytoplankton, *Annu. Rev. Mar. Sci.*, 5, 217–246, doi:10.1146/annurev-marine-121211-172356,
21 2013.
- 22 Behrenfeld, M. J., Prasil, O., Babin, M. and Bruyant, F.: In search of a physiological basis for
23 covariations in light-limited and light-saturated photosynthesis, *J. Phycol.*, 40, 4–25, 2004.
- 24 Behrenfeld, M. J., Halsey, K. H. and Milligan, A. J.: Evolved physiological responses of
25 phytoplankton to their integrated growth environment, *Philos. Trans. R. Soc. B Biol. Sci.*, 363,
26 2687–2703, 2008.
- 27 Bilger, W. and Björkman, O.: Role of the xanthophyll cycle in photoprotection elucidated by
28 measurements of light-induced absorbance changes, fluorescence and photosynthesis in leaves of
29 *Hedera canariensis*, *Photosynth. Res.*, 25, 173–185, doi:10.1007/BF00033159, 1990.
- 30 Brunet, C., Johnsen, G., Lavaud, J. and Roy, S.: Pigments and photoacclimation processes,
31 *Phytoplankton Pigments Charact. Chemotaxon. Appl. Oceanogr.*, available at:
32 <https://hal.archives-ouvertes.fr/hal-01101814/> (last accessed 14 December 2015), 2011.
- 33 Bruyant, F., Babin, M., Genty, B., Prasil, O., Behrenfeld, M. J., Claustre, H., Bricaud, A.,
34 Garczarek, L., Holtzendorff, J. and Koblizek, M.: Diel variations in the photosynthetic
35 parameters of *Prochlorococcus* strain PCC 9511: Combined effects of light and cell cycle,
36 *Limnol. Oceanogr.*, 50, 850–863, 2005.

- 37 Cardol, P., Forti, G. and Finazzi, G.: Regulation of electron transport in microalgae, *Biochim.*
38 *Biophys. Acta BBA-Bioenerg.*, 1807, 912–918, 2011.
- 39 Cheah, W., McMinn, A., Griffiths, F. B., Westwood, K. J., Wright, S. W., Molina, E., Webb, J.
40 P. and van den Enden, R.: Assessing sub-antarctic zone primary productivity from fast repetition
41 rate fluorometry, *Deep Sea Res. Part II Top. Stud. Oceanogr.*, 58, 2179–2188,
42 doi:10.1016/j.dsr2.2011.05.023, 2011.
- 43 Corno, G., Letelier, R. M., Abbott, M. R. and Karl, D. M.: Assessing primary production
44 variability in the North Pacific Subtropical Gyre: a comparison of fast repetition rate fluorometry
45 and ¹⁴C measurements, *J. Phycol.*, 42, 51–60, 2006.
- 46 Demmig-Adams, B., Garab, G., Adams III, W. and Govindjee (Eds.): *Non-Photochemical*
47 *Quenching and Energy Dissipation in Plants, Algae and Cyanobacteria*, Springer Netherlands,
48 Dordrecht. Available from: <http://link.springer.com/10.1007/978-94-017-9032-1> (last accessed 9
49 June 2015), 2014.
- 50 Derks, A., Schaven, K. and Bruce, D.: Diverse mechanisms for photoprotection in
51 photosynthesis. Dynamic regulation of photosystem II excitation in response to rapid
52 environmental change, *Biochim. Biophys. Acta BBA - Bioenerg.*, 1847, 468–485,
53 doi:10.1016/j.bbabi.2015.02.008, 2015.
- 54 Doblin, M. A., Petrou, K. L., Shelly, K., Westwood, K., van den Enden, R., Wright, S., Griffiths,
55 B. and Ralph, P. J.: Diel variation of chlorophyll-*a* fluorescence, phytoplankton pigments and
56 productivity in the Sub-Antarctic and Polar Front Zones south of Tasmania, Australia, *Deep Sea*
57 *Res. Part II Top. Stud. Oceanogr.*, 58, 2189–2199, doi:10.1016/j.dsr2.2011.05.021, 2011.
- 58 Doty, M. S. and Oguri, M.: Evidence for a photosynthetic daily periodicity, *Limnol. Oceanogr.*,
59 2, 37–40, doi:10.4319/lm.1957.2.1.0037, 1957.
- 60 Erga, S. R. and Skjoldal, H. R.: Diel variations in photosynthetic activity of summer
61 phytoplankton in Linda aspollene, western Norway, Available from:
62 <http://brage.bibsys.no/xmlui/handle/11250/108310> (last accessed 14 December 2015), 1990.
- 63 Feikema, O. W., Marosvölgyi, M. A., Lavaud, J. and van Gorkom, H. J.: Cyclic electron transfer
64 in photosystem II in the marine diatom *Phaeodactylum tricornutum*, *Biochim. Biophys. Acta*
65 *BBA - Bioenerg.*, 1757, 829–834, doi:10.1016/j.bbabi.2006.06.003, 2006.
- 66 Field, C. B., Behrenfeld, M. J., Randerson, J. T. and Falkowski, P.: Primary production of the
67 biosphere: integrating terrestrial and oceanic components, *Science*, 281, 237–240, 1998.
- 68 Foyer, C. H., Bloom, A. J., Queval, G. and Noctor, G.: Photorespiratory metabolism: genes,
69 mutants, energetics, and redox signaling, *Annu. Rev. Plant Biol.*, 60, 455–484,
70 doi:10.1146/annurev.arplant.043008.091948, 2009.
- 71 From, N., Richardson, K., Mousing, E. A. and Jensen, P. E.: Removing the light history signal
72 from normalized variable fluorescence (F_v/F_m) measurements on marine phytoplankton, *Limnol.*
73 *Oceanogr. Methods*, 12, 776–783, doi:10.4319/lom.2014.12.776, 2014.

- 74 Fujiki, T., Suzue, T., Kimoto, H. and Saino, T.: Photosynthetic electron transport in *Dunaliella*
75 *tertiolecta* (Chlorophyceae) measured by fast repetition rate fluorometry: relation to carbon
76 assimilation, *J. Plankton Res.*, 29, 199–208, 2007.
- 77 Giordano, M., Beardall, J. and Raven, J. A.: CO₂ Concentrating mechanisms in algae:
78 mechanisms, environmental modulation, and evolution, *Annu. Rev. Plant Biol.*, 56, 99–131,
79 doi:10.1146/annurev.arplant.56.032604.144052, 2005.
- 80 Goto, N., Miyazaki, H., Nakamura, N., Terai, H., Ishida, N. and Mitamura, O.: Relationships
81 between electron transport rates determined by pulse amplitude modulated (PAM) chlorophyll
82 fluorescence and photosynthetic rates by traditional and common methods in natural freshwater
83 phytoplankton, *Fundam. Appl. Limnol. Arch. Fr Hydrobiol.*, 172, 121–134, doi:10.1127/1863-
84 9135/2008/0172-0121, 2008.
- 85 Granum, E., Roberts, K., Raven, J. A. and Leegood, R. C.: Primary carbon and nitrogen
86 metabolic gene expression in the diatom *Thalassiosira pseudonana* (bacillariophyceae): diel
87 periodicity and effects of inorganic carbon and nitrogen1, *J. Phycol.*, 45, 1083–1092,
88 doi:10.1111/j.1529-8817.2009.00728.x, 2009.
- 89 Halsey, K. H. and Jones, B. M.: Phytoplankton strategies for photosynthetic energy allocation,
90 *Annu. Rev. Mar. Sci.*, 7, 265–297, doi:10.1146/annurev-marine-010814-015813, 2015.
- 91 Halsey, K. H., Milligan, A. J. and Behrenfeld, M. J.: Linking time-dependent carbon-fixation
92 efficiencies in *Dunaliella tertiolecta* (chlorophyceae) to underlying metabolic pathways, *J.*
93 *Phycol.*, 47, 66–76, doi:10.1111/j.1529-8817.2010.00945.x, 2011.
- 94 Harding, L. W., Meeson, B. W., Prézelin, B. B. and Sweeney, B. M.: Diel periodicity of
95 photosynthesis in marine phytoplankton, *Mar. Biol.*, 61, 95–105, doi:10.1007/BF00386649,
96 1981.
- 97 Harding, L. W., Prézelin, B. B., Sweeney, B. M. and Cox, J. L.: Primary production as
98 influenced by diel periodicity of phytoplankton photosynthesis, *Mar. Biol.*, 67, 179–186, 1982.
- 99 Harding, L. W., Fisher, T. R. and Tyler, M. A.: Adaptive responses of photosynthesis in
100 phytoplankton: specificity to time-scale of change in light, *Biol. Oceanogr.*, 4, 403–437,
101 doi:10.1080/01965581.1987.10749499, 1987.
- 102 John, D. E., López-Díaz, J. M., Cabrera, A., Santiago, N. A., Corredor, J. E., Bronk, D. A. and
103 Paul, J. H.: A day in the life in the dynamic marine environment: how nutrients shape diel
104 patterns of phytoplankton photosynthesis and carbon fixation gene expression in the Mississippi
105 and Orinoco River plumes, *Hydrobiologia*, 679, 155–173, 2012.
- 106 Kaiblinger, C. and Dokulil, M. T.: Application of fast repetition rate fluorometry to
107 phytoplankton photosynthetic parameters in freshwaters, *Photosynth. Res.*, 88, 19–30, 2006.
- 108 Kirk, J. T. O.: *Light and Photosynthesis in Aquatic Ecosystems*, Cambridge University Press,
109 Cambridge, UK, 2011.

- 110 Kishino, M., Takahashi, M., Okami, N. and Ichimura, S.: Estimation of the spectral absorption
111 coefficients of phytoplankton in the sea, *Bull. Mar. Sci.*, 37, 634–642, 1985.
- 112 Knap, A. H., Michaels, A., Close, A. R., Ducklow, H. and Dickson, A. G.: Protocols for the joint
113 global ocean flux study (JGOFS) core measurements, JGOFS Repr. IOC Man. Guid. No 29
114 UNESCO 1994, 19, available from: <http://epic.awi.de/17559/1/Kna1996a.pdf> (Accessed 15
115 October 2014), 1996.
- 116 Kolber, Z. and Falkowski, P. G.: Use of active fluorescence to estimate phytoplankton
117 photosynthesis in situ, *Limnol. Oceanogr.*, 38, 1646–1665, doi:10.2307/2838443, 1993.
- 118 Kolber, Z. S., Prášil, O. and Falkowski, P. G.: Measurements of variable chlorophyll
119 fluorescence using fast repetition rate techniques: defining methodology and experimental
120 protocols, *Biochim. Biophys. Acta BBA - Bioenerg.*, 1367, 88–106, doi:10.1016/S0005-
121 2728(98)00135-2, 1998.
- 122 Laureau, C., DE Paepe, R., Latouche, G., Moreno-Chacón, M., Finazzi, G., Kuntz, M., Cornic,
123 G. and Streb, P.: Plastid terminal oxidase (PTOX) has the potential to act as a safety valve for
124 excess excitation energy in the alpine plant species *Ranunculus glacialis*, *Plant Cell Environ.*,
125 doi:10.1111/pce.12059, 2013.
- 126 Lawrenz, E., Silsbe, G., Capuzzo, E., Ylöstalo, P., Forster, R. M., Simis, S. G. H., Prášil, O.,
127 Kromkamp, J. C., Hickman, A. E., Moore, C. M., Forget, M.-H., Geider, R. J. and Suggett, D. J.:
128 Predicting the electron requirement for carbon fixation in seas and oceans, *PLoS ONE*, 8,
129 e58137, doi:10.1371/journal.pone.0058137, 2013.
- 130 Laws, E. A.: Photosynthetic quotients, new production and net community production in the
131 open ocean, *Deep Sea Res. Part Oceanogr. Res. Pap.*, 38, 143–167, 1991.
- 132 Lee, Y. W., Park, M. O., Kim, Y. S., Kim, S. S. and Kang, C. K.: Application of photosynthetic
133 pigment analysis using a HPLC and CHEMTAX program to studies of phytoplankton
134 community composition, *J Korean Soc Ocean.*, 16, 117–124, 2011.
- 135 MacCaull, W. A. and Platt, T.: Diel variations in the photosynthetic parameters of coastal marine
136 phytoplankton, *Limnol. Oceanogr.*, 22, 723–731, doi:10.4319/lo.1977.22.4.0723, 1977.
- 137 Mackey, K. R. M., Paytan, A., Grossman, A. R. and Bailey, S.: A photosynthetic strategy for
138 coping in a high-light, low-nutrient environment, *Limnol. Oceanogr.*, 53, 900–913,
139 doi:10.4319/lo.2008.53.3.0900, 2008.
- 140 McDonald, A. E., Ivanov, A. G., Bode, R., Maxwell, D. P., Rodermel, S. R. and Hüner, N. P. A.:
141 Flexibility in photosynthetic electron transport: The physiological role of plastoquinol terminal
142 oxidase (PTOX), *Biochim. Biophys. Acta BBA - Bioenerg.*, 1807, 954–967,
143 doi:10.1016/j.bbabo.2010.10.024, 2011.
- 144 McKew, B. A., Davey, P., Finch, S. J., Hopkins, J., Lefebvre, S. C., Metodiev, M. V.,
145 Oxborough, K., Raines, C. A., Lawson, T. and Geider, R. J.: The trade-off between the light-
146 harvesting and photoprotective functions of fucoxanthin-chlorophyll proteins dominates light

- 147 acclimation in *Emiliana huxleyi* (clone CCMP 1516), *New Phytol.*, 200, 74–85,
148 doi:10.1111/nph.12373, 2013.
- 149 Milligan, A. J., Halsey, K. H. and Behrenfeld, M. J.: Advancing interpretations of ¹⁴C-uptake
150 measurements in the context of phytoplankton physiology and ecology, *J. Plankton Res.*, 37,
151 692–698, doi:10.1093/plankt/fbv051, 2015.
- 152 Mitchell, B. G., Kahru, M., Wieland, J. and Stramska, M.: Determination of spectral absorption
153 coefficients of particles, dissolved material and phytoplankton for discrete water samples, *Ocean*
154 *Opt. Protoc. Satell. Ocean Color Sens. Valid. Revis.*, 3, 231–257, 2002.
- 155 Miyake, C. and Asada, K.: The Water-Water Cycle in Algae, in *Photosynthesis in Algae*, edited
156 by Larkum A. W. D., Douglas S. E., and Raven J. A., 183–204, Springer, Netherlands, available
157 from: http://link.springer.com/chapter/10.1007/978-94-007-1038-2_9 (Accessed 10 March
158 2015), 2003.
- 159 Morel, A., Gentili, B., Claustre, H., Babin, M., Bricaud, A., Ras, J. and Tièche, F.: Optical
160 properties of the “clearest” natural waters, *Limnol. Oceanogr.*, 52, 217–229,
161 doi:10.4319/lo.2007.52.1.0217, 2007.
- 162 Myers, J.: On the algae: thoughts about physiology and measurements of efficiency, in *Primary*
163 *Productivity in the Sea*, edited by Falkowski, P. G., 1–16, Springer, New York, US, available at:
164 http://link.springer.com/chapter/10.1007/978-1-4684-3890-1_1 (Accessed 28 August 2015),
165 1980.
- 166 Napoléon, C. and Claquin, P.: Multi-parametric relationships between PAM measurements and
167 carbon incorporation, an in situ approach, *PloS One*, 7, e40284,
168 doi:10.1371/journal.pone.0040284, 2012.
- 169 Napoléon, C., Raimbault, V. and Claquin, P.: Influence of nutrient stress on the relationships
170 between PAM measurements and carbon incorporation in four phytoplankton species., *PloS One*,
171 8, e66423, doi:10.1371/journal.pone.0066423, 2013.
- 172 Nawrocki, W. J., Tourasse, N. J., Taly, A., Rappaport, F. and Wollman, F.-A.: The plastid
173 terminal oxidase: its elusive function points to multiple contributions to plastid physiology,
174 *Annu. Rev. Plant Biol.*, 66, 49–74, doi:10.1146/annurev-arplant-043014-114744, 2015.
- 175 Niyogi, K. K.: Safety valves for photosynthesis, *Curr. Opin. Plant Biol.*, 3, 455–460,
176 doi:10.1016/S1369-5266(00)00113-8, 2000.
- 177 Öquist, G., Chow, W. S. and Anderson, J. M.: Photoinhibition of photosynthesis represents a
178 mechanism for the long-term regulation of photosystem II, *Planta*, 186, 450–460,
179 doi:10.1007/BF00195327, 1992.
- 180 Ottesen, E. A., Young, C. R., Gifford, S. M., Eppley, J. M., Marin, R., Schuster, S. C., Scholin,
181 C. A. and DeLong, E. F.: Multispecies diel transcriptional oscillations in open ocean
182 heterotrophic bacterial assemblages, *Science*, 345, 207–212, doi:10.1126/science.1252476, 2014.

183 Oxborough, K. and Baker, N. R.: Resolving chlorophyll a fluorescence images of photosynthetic
184 efficiency into photochemical and non-photochemical components – calculation of qP and
185 F_v'/F_m' without measuring F_o' ; Photosynth. Res., 54, 135–142, doi:10.1023/A:1005936823310,
186 1997.

187 Oxborough, K., Moore, C. M., Suggett, D. J., Lawson, T., Chan, H. G. and Geider, R. J.: Direct
188 estimation of functional PSII reaction center concentration and PSII electron flux on a volume
189 basis: a new approach to the analysis of Fast Repetition Rate fluorometry (FRRf) data, Limnol
190 Ocean. Methods, 10, 142–154, 2012.

191 Pei, S. and Laws, E. A.: Does the ^{14}C method estimate net photosynthesis? Implications from
192 batch and continuous culture studies of marine phytoplankton, Deep Sea Res. Part Oceanogr.
193 Res. Pap., 82, 1–9, doi:10.1016/j.dsr.2013.07.011, 2013.

194 Pinckney, J. L.: HPLC Method - Technical - Estuarine Ecology, available from:
195 <https://sites.google.com/site/jaypinckney/home/protocols-reports> (last accessed 14 December
196 2015), 2013.

197 Pope, R. M. and Fry, E. S.: Absorption spectrum (380–700 nm) of pure water. II. Integrating
198 cavity measurements, Appl. Opt., 36, 8710, doi:10.1364/AO.36.008710, 1997.

199 Prasil, O., Kolber, Z., Berry, J. A. and Falkowski, P. G.: Cyclic electron flow around
200 photosystem II in vivo; Photosynth. Res., 48, 395–410, doi:10.1007/BF00029472, 1996.

201 Prézelin, B. B.: Diel periodicity in phytoplankton productivity, Hydrobiologia, 238, 1–35, 1992.

202 Raateoja, M. P.: Fast repetition rate fluorometry (FRRF) measuring phytoplankton productivity:
203 a case study at the entrance to the Gulf of Finland, Baltic Sea, Boreal Environ. Res., 9, 263–276,
204 2004.

205 Raven, J. A., Evans, M. C. W. and Korb, R. E.: The role of trace metals in photosynthetic
206 electron transport in O_2 -evolving organisms, Photosynth. Res., 60, 111–150,
207 doi:10.1023/A:1006282714942, 1999.

208 Ribalet, F., Swalwell, J., Clayton, S., Jiménez, V., Sudek, S., Lin, Y., Johnson, Z. I., Worden, A.
209 Z. and Armbrust, E. V.: Light-driven synchrony of *Prochlorococcus* growth and mortality in the
210 subtropical Pacific gyre, Proc. Natl. Acad. Sci., 201424279, doi:10.1073/pnas.1424279112,
211 2015.

212 Roháček, K.: Chlorophyll fluorescence parameters: the definitions, photosynthetic meaning, and
213 mutual relationships, Photosynthetica, 40, 13–29, doi:10.1023/A:1020125719386, 2002.

214 Röttgers, R. and Gehnke, S.: Measurement of light absorption by aquatic particles: improvement
215 of the quantitative filter technique by use of an integrating sphere approach, Appl. Opt., 51,
216 1336–1351, 2012.

- 217 Schrader, P. S., Milligan, A. J. and Behrenfeld, M. J.: Surplus photosynthetic antennae
218 complexes underlie diagnostics of iron limitation in a cyanobacterium, PLoS ONE, 6, e18753,
219 doi:10.1371/journal.pone.0018753, 2011.
- 220 Schreiber, U.: Pulse-amplitude-modulation (PAM) fluorometry and saturation pulse method: an
221 overview, Chlorophyll Fluoresc., 19, 279–319, 2004.
- 222 Schuback, N., Schallenberg, C., Duckham, C., Maldonado, M. T. and Tortell, P. D.: Interacting
223 effects of light and iron availability on the coupling of photosynthetic electron transport and
224 CO₂-assimilation in marine phytoplankton, PLoS ONE, 10, e0133235,
225 doi:10.1371/journal.pone.0133235, 2015.
- 226 Silsbe, G.: Phytotools: Phytoplankton Production Tools, an R package available on CRAN:
227 <https://cran.r-project.org/web/packages/phytotools/index.html>, 2015.
- 228 Streb, P., Josse, E.-M., Gallouët, E., Baptist, F., Kuntz, M. and Cornic, G.: Evidence for
229 alternative electron sinks to photosynthetic carbon assimilation in the high mountain plant
230 species *Ranunculus glacialis*, Plant Cell Environ., 28, 1123–1135, doi:10.1111/j.1365-
231 3040.2005.01350.x, 2005.
- 232 Stross, R. G., Chisholm, S. W. and Downing, T. A.: Causes of daily rhythms in photosynthetic
233 rates of phytoplankton, Biol. Bull., 145, 200–209, doi:10.2307/1540359, 1973.
- 234 Suggett, D., Kraay, G., Holligan, P., Davey, M., Aiken, J. and Geider, R.: Assessment of
235 photosynthesis in a spring cyanobacterial bloom by use of a fast repetition rate fluorometer,
236 Limnol. Oceanogr., 46, 802–810, 2001.
- 237 Suggett, D. J., Maberly, S. C. and Geider, R. J.: Gross photosynthesis and lake community
238 metabolism during the spring phytoplankton bloom, Limnol. Oceanogr., 51, 2064–2076, 2006.
- 239 Suggett, D. J., Moore, C. M., Hickman, A. E. and Geider, R. J.: Interpretation of fast repetition
240 rate (FRR) fluorescence: signatures of phytoplankton community structure versus physiological
241 state, Mar Ecol Prog Ser, 376, 1–19, 2009.
- 242 Suggett, D. J., Moore, C. M. and Geider, R. J.: Estimating aquatic productivity from active
243 fluorescence measurements, in: Chlorophyll *a* Fluorescence in Aquatic Sciences: Methods and
244 Applications, edited by: Suggett D. J., Prasil O., and Borowitzka M. A., 103–127, Springer, the
245 Netherlands, 2010.
- 246 Suzuki, L. and Johnson, C. H.: Algae know the time of day: circadian and photoperiodic
247 programs, J. Phycol., 37, 933–942, doi:10.1046/j.1529-8817.2001.01094.x, 2001.
- 248 Taylor, R. L., Semeniuk, D. M., Payne, C. D., Zhou, J., Tremblay, J.-É., Cullen, J. T. and
249 Maldonado, M. T.: Colimitation by light, nitrate, and iron in the Beaufort Sea in late summer, J.
250 Geophys. Res. Oceans, 118, 3260–3277, doi:10.1002/jgrc.20244, 2013.

251 Vass, I.: Role of charge recombination processes in photodamage and photoprotection of the
252 photosystem II complex, *Physiol. Plant.*, 142, 6–16, doi:10.1111/j.1399-3054.2011.01454.x,
253 2011.

254 Vassiliev, I. R., Kolber, Z., Wyman, K. D., Mauzerall, D., Shukla, V. K. and Falkowski, P. G.:
255 Effects of iron limitation on photosystem II composition and light utilization in *Dunaliella*
256 *tertiolecta*, *Plant Physiol.*, 109, 963–972, doi:10.1104/pp.109.3.963, 1995.

257 Webb, W. L., Newton, M. and Starr, D.: Carbon Dioxide Exchange of *Alnus rubra*. A
258 Mathematical Model, *Oecologia*, 17, 281–291, 1974.

259 Welschmeyer, N. A.: Fluorometric analysis of chlorophyll *a* in the presence of chlorophyll *b* and
260 pheopigments, *Limnol. Oceanogr.*, 39, 1985–1992, 1994.

261 Williams, P. J. le B., Thomas, D. N. and Reynolds, C. S.: *Phytoplankton Productivity: Carbon*
262 *Assimilation in Marine and Freshwater Ecosystems*, John Wiley and Sons., 2008.

263 Yruela, I.: Transition metals in plant photosynthesis, *Met. Integr. Biometal Sci.*, 5, 1090–1109,
264 doi:10.1039/c3mt00086a, 2013.

265 Zehr, J. P. and Kudela, R. M.: Photosynthesis in the Open Ocean, *Science*, 326, 945–946,
266 doi:10.1126/science.1181277, 2009.

267 Zhao, Y. and Quigg, A.: Study of photosynthetic productivity in the Northern Gulf of Mexico:
268 Importance of diel cycles and light penetration, *Cont. Shelf Res.*, 102, 33–46,
269 doi:10.1016/j.csr.2015.04.014, 2015.

270

271

272

273

274

275

276

277

278

279

280

281

282

283

284

285 **Tables and Figures**

286

287 **Table 1: Parameters measures at each time-point during the diurnal experiment.**

Time Point	1	2	3	4	5	6	7	8
Local time	3:00	6:00	9:00	12:00	15:00	18:00	21:00	0:00
[chl _a]	x	x	x	x	x	x	x	x
HPLC	x		x		x		x	
Absorption Spectra	x	x	x	x	x	x	x	x
FRRF measurements	x	x	x	x	x	x	x	x
C-fixation	x	x	x	x	x	x	x	x

288

289

290

291 **Table 2: Phytoplankton pigments used for the derivation of diagnostic pigment ratios.**

292 Pigments identified from HPLC analysis were chlorophyll *c*₃ (Chl *c*₃), chlorophyll *c*₁*c*₂ (Chl
293 *c*₁*c*₂), 19'butanoyloxyfucoxanthin (19'ButFuc), fucoxanthin (Fuco), 19'hexanoyloxyfucoxanthin
294 (19'HexFuc), 9'cis-neoxanthin (Neo), prasinoxanthin (Prasino), violaxanthin (Viola),
295 diadinoxanthin (Dd), alloxanthin (Allox), diatoxanthin (Dt), lutein, zeaxanthin (Zea), chlorophyll
296 *b* (Chl *b*), chlorophyll *a* allomer (Chl *a* allomer), chlorophyll *a* + divinyl chlorophyll *a* (Chl *a*),
297 chlorophyll *a*' (Chl *a* prime), α carotene (α carot), β carotene (β carot).

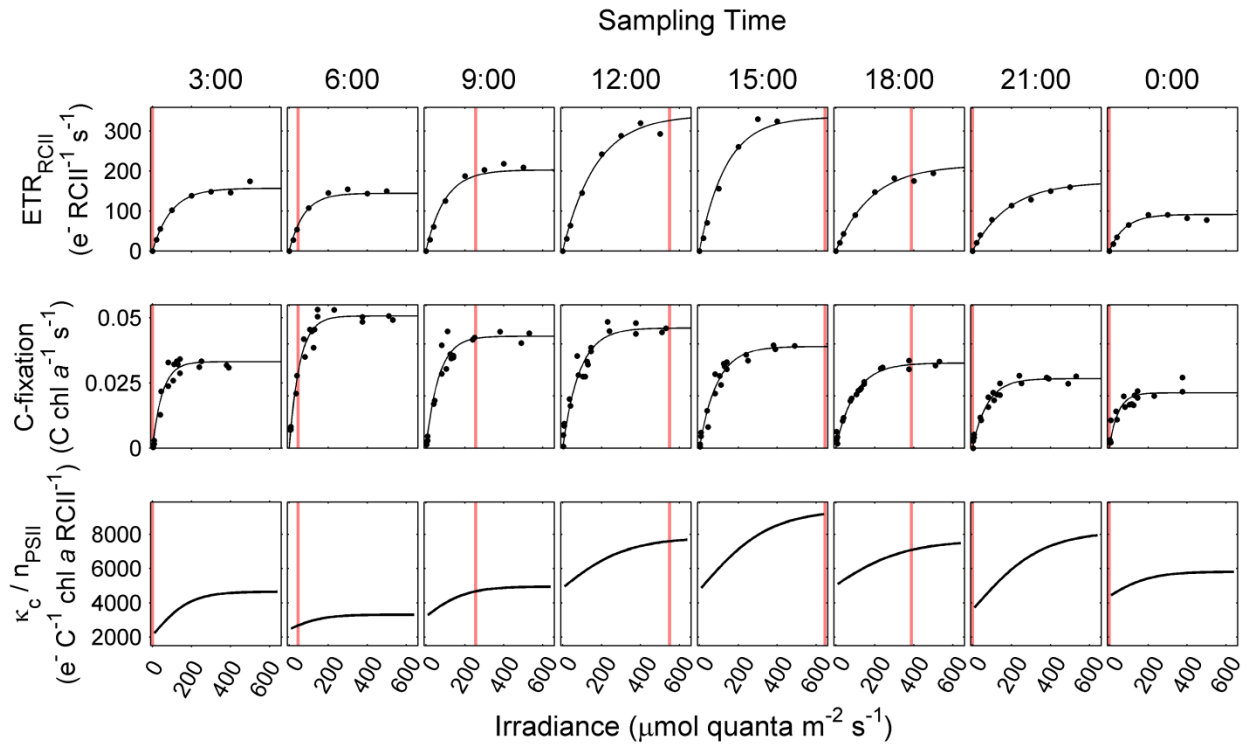
Pigment group	Pigments
Photoprotective carotenoids (PPC)	Neo + Viola + Dd + Allox + Dt + Lutein + Zea + β carot
Photosynthetic carotenoids (PSC)	19'ButFuc + Fuco + 19'HexFuc + Prasino + α carot
Total chlorophyll (Tchl)	Chl <i>c</i> ₃ + Chl <i>c</i> ₁ <i>c</i> ₂ + Chl <i>b</i> + Chl <i>a</i> allomer + Chl <i>a</i> + Chl <i>a</i> prime
Total pigment (TPig)	PPC + PSC + Tchl

298

299

300

301



303

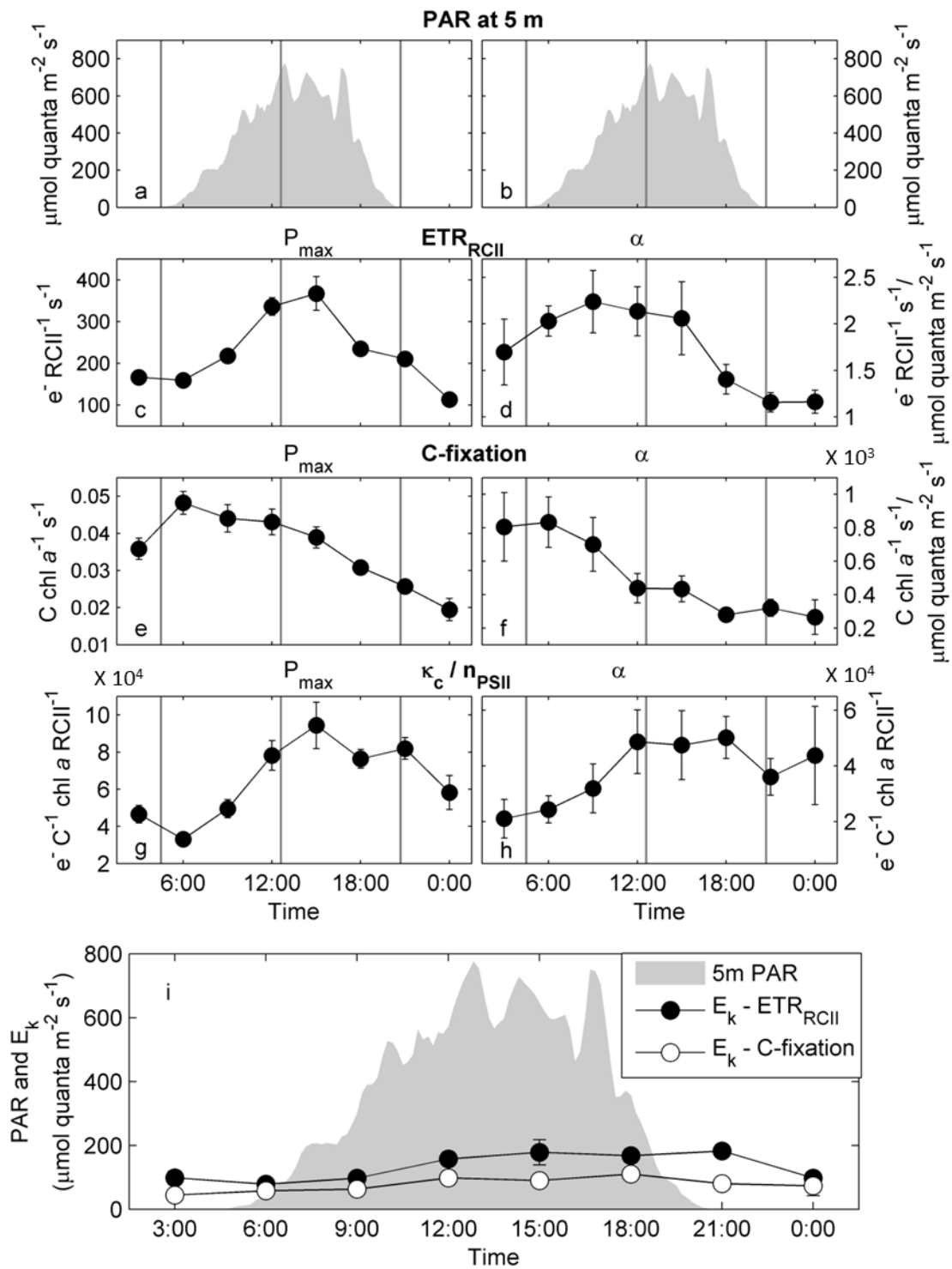
304 **Figure 1: Diurnal variation in rates and light dependency of ETR_{RCII} , carbon fixation and**305 **the derived conversion factor K_c/n_{PSII} .** PvsE curves of ETR_{RCII} ($\text{mol e}^- \text{mol RCI}^{-1} \text{s}^{-1}$) and306 carbon fixation ($\text{mol C mol chl } a^{-1} \text{s}^{-1}$) were measured at 3 hour intervals over a 24 hour diurnal

307 cycle. Data were fit to the exponential model of Webb et al. (1974). The conversion factor

308 K_c/n_{PSII} ($\text{mol e}^- \text{mol C}^{-1} \text{mol chl } a \text{mol RCI}^{-1}$), and its light dependency, were derived as the309 quotient of corresponding values of ETR_{RCII} and carbon fixation. The vertical line on plots

310 corresponds to in situ PAR values at 5 m depth during sampling for each time-point.

311



312

313 **Figure 2: Diurnal changes in capacities and efficiencies of $E_{\text{TR}_{\text{RCII}}}$ and carbon fixation and**

314 **the derived conversion factor $\kappa_{\text{c}}/n_{\text{PSII}}$. The conversion factor $\kappa_{\text{c}}/n_{\text{PSII}}$ at light saturation (g) is**

315 **derived from the values in (c) and (e). Similarly, the conversion factor $\kappa_{\text{c}}/n_{\text{PSII}}$ under light**

316 limiting conditions (h) is derived from values in (d) and (f). The error in (b), (c), (e), and (f) is
317 the 95% confidence interval of the parameter derived from the fit to data shown in Fig. 1, and the
318 error in (d) and (g) is the propagated error for (b)/(c) and (e)/(f), respectively. PAR at 5 m depth
319 is shown in (a) and (b). The vertical gray lines in panel (a-h) mark sunrise, solar noon and sunset.
320 Panel (i) shows the light saturation parameter E_k for ETR_{RCII} and carbon fixation in relation to in
321 situ light availability.

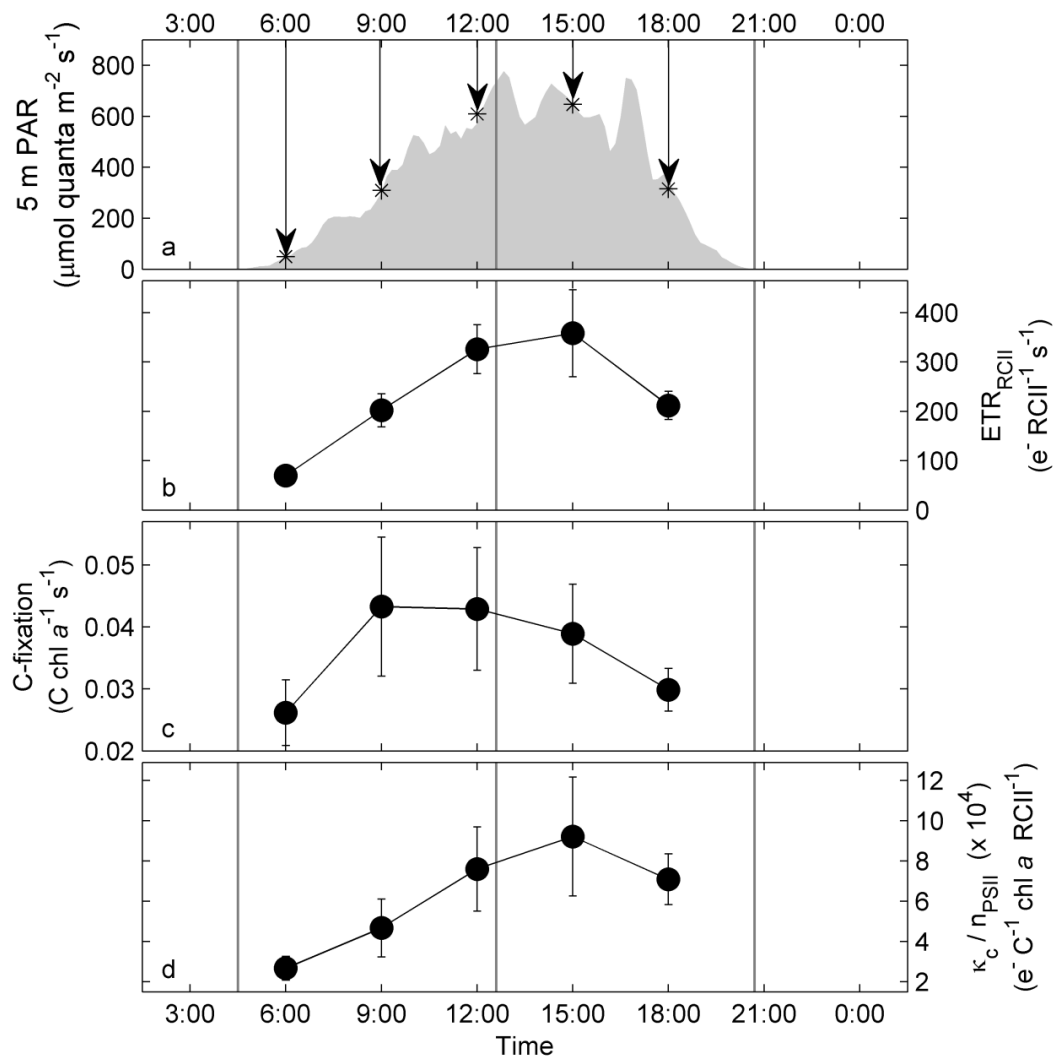
322

323

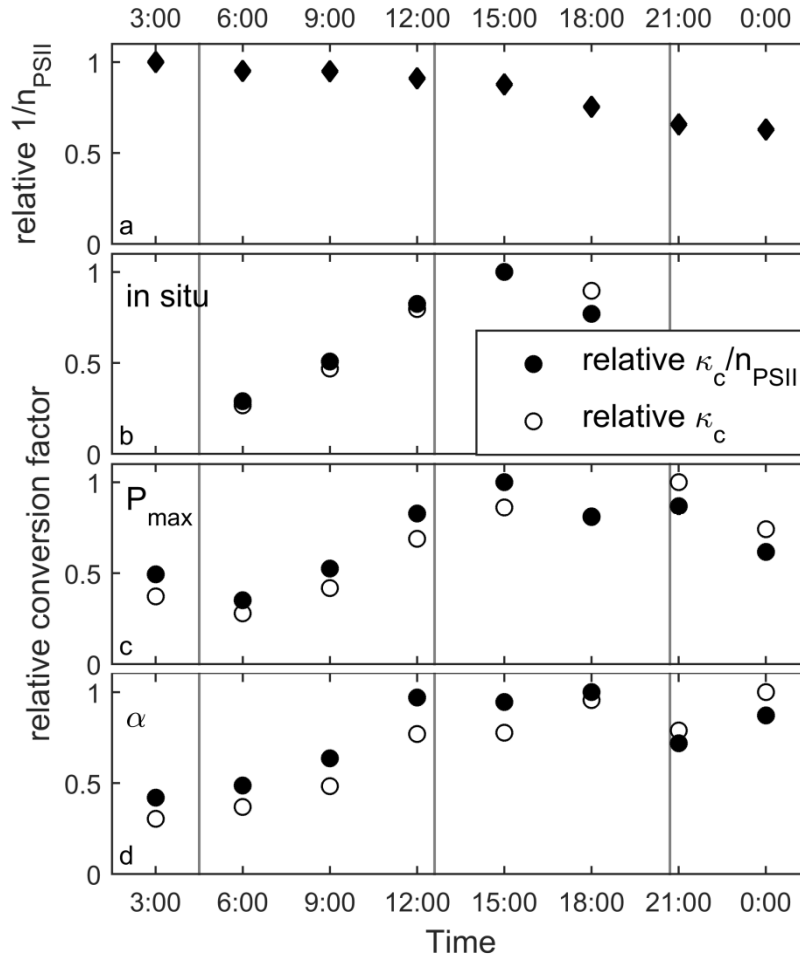
324

325

326

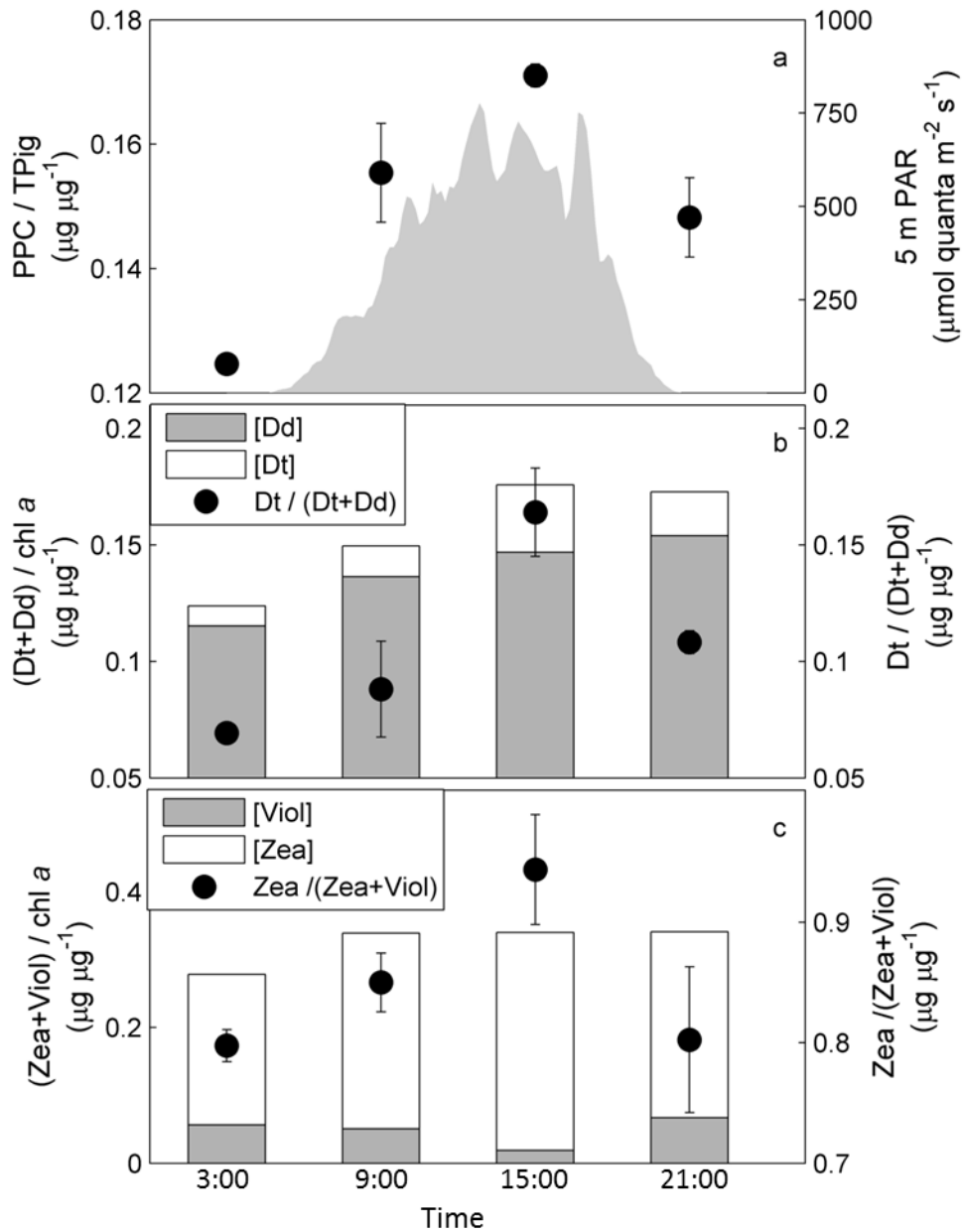


327
 328 **Figure 3: Diurnal changes in ETR_{RCII} , carbon fixation and κ_c/n_{PSII} derived for in situ light**
 329 **intensities at 5 m depth.** Diurnal changes in irradiance at 5 m depth (a), with arrows indicating
 330 the PAR value used to derive rates in (b) and (c). Realized rates of ETR_{RCII} (b) and carbon
 331 fixation (c) at each time-point were derived from the P_{vsE} relationship established in Fig. 1. The
 332 error in (b) and (c) is the propagated 95% confidence interval of the parameter P_{vsE} fit
 333 parameters, and the error in (d) is the propagated error from (b)/(c). The vertical gray lines in all
 334 plots mark sunrise, solar noon and sunset.



335

336 Figure 4: Relative changes in the components of our conversion factor K_c/n_{PSII} over the diurnal
 337 cycle. Panel (a) shows diurnal changes in $1/n_{PSII}$ (mol chl *a* mol RCII⁻¹), estimated as
 338 $(F_0/\sigma_{PSII})/[chl\ a]$. These relative values of $1/n_{PSII}$ were then used to derive relative values of K_c
 339 (mol e⁻ mol C⁻¹) from values of K_c/n_{PSII} . This was done for the conversion factor derived for in
 340 situ irradiances at 5 m depth (b), the conversion factor derived for light saturated rates (c) and the
 341 conversion factor for light limited rates (d). All values are scaled to 1 for clarity.

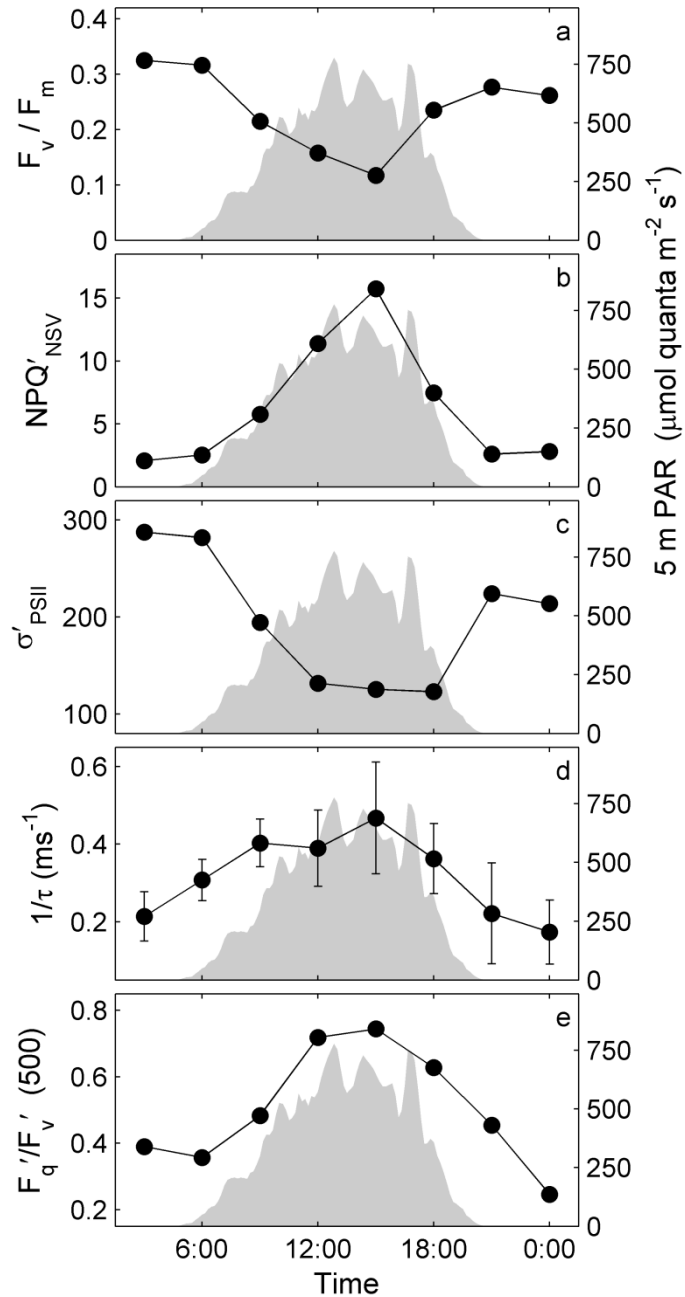


342

343 **Figure 5: Diurnal changes in pigment ratios.** Panel (a) shows changes in the abundance of all
 344 photoprotective pigment (PPC), relative to the total pigment present (TPig) at each time-point.
 345 See Table 2 for a definition of pigment groups used to derive these ratios. Panel (b) shows
 346 relative changes in the abundance of the chromophyte xanthophyll cycling pigments Dd and Dt,
 347 normalized to [chl *a*]. Changes in the de-epoxidation state ration (DES ratio = Dt/(Dt+Dd)), also
 348 shown in (b), indicate the extent of active photo-protective energy dissipation through
 349 xanthophyll cycling in the pigment antenna. Similarly, panel (c) shows xanthophyll cycling

350 pigments Viol and Zea, specific to prasinophytes and chlorophytes. Error bars are the range of
351 values from two replicate samples taken at each time-point.

352

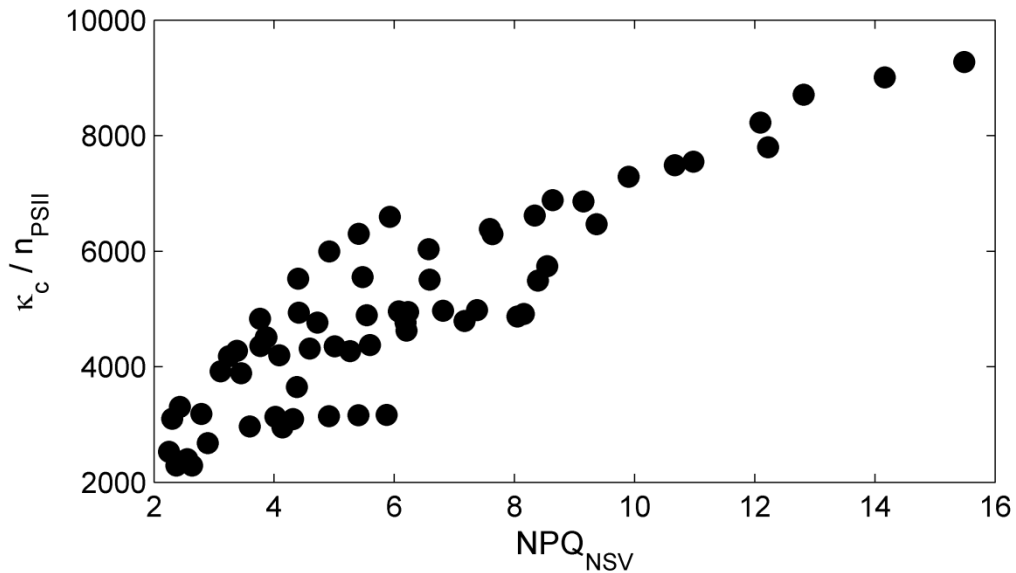


353

354 **Figure 6: Diurnal changes in PSII photophysiological parameters derived from FRRF**
355 **measurements.** Panel (a) F_v/F_m in the dark-regulated state at each TP. Panel (b) and (c) show the

356 normalized Stern-Volmer quenching, NPQ_{NSV} , derived as F_o'/F_v' (McKew et al., 2013) and the
357 functional absorption cross section, σ'_{PSII} , both estimated for in situ light availability at each TP.
358 Values in (b) and (c) were calculated by extrapolating between values derived for each light step
359 of the FRRF steady state light curves. Panel (d) shows estimates of the rate of re-oxidation of
360 Q_A . Panel (c) shows estimates of photochemical quenching (F_q'/F_v'), indicating the fraction of
361 open RCII (primary stable electron acceptor Q_A oxidized) at a reference irradiance level of 500
362 $\mu\text{mol quanta m}^{-2}\text{s}^{-1}$.

363



364

365 **Figure 7: Correlation between the conversion factor K_c/n_{PSII} and the expression of NPQ_{NSV} .**

366 NPQ_{NSV} was derived as F_o'/F_v' (McKew et al., 2013), for each step of the FRRF light curve at

367 each TP. Values of K_c/n_{PSII} corresponding to the same light intensities were derived by

368 extrapolation along the carbon fixation and ETR_{RCII} based P_{vsE} curves.